



COMPLETE AND INCOMPLETE FUSION STUDIES
IN SOME $^{14}\text{N} + ^{59}\text{Co}$ SYSTEMS

By

Biniyam Nigussie

A THESIS SUBMITTED TO THE SCHOOL OF GRADUATE
STUDIES OF ADDIS ABABA UNIVERSITY IN PARTIAL
FULFILLMENT OF THEREQUIREMENTS FOR THE DEGREE OF
MASTER OF SCIENCE IN PHYSICS

AT

ADDIS ABABA UNIVERSITY

ADDIS ABABA, ETHIOPIA

JUNE, 2012

© Copy right by Biniyam Nigussie, 2012

ADDIS ABABA UNIVERSITY
DEPARTMENT OF
PHYSICS

Advisor:

Prof.A.K. Chaubey

Examiner:

Dr.S. Bhatnagar

Examiner:

Dr. Tilahun Tesfaye

ADDIS ABABA UNIVERSITY

Date: **JUNE 2012**

Author: **Biniyam Nigussie**

TITLE: **COMPLETE AND INCOMPLETE FUSION STUDIES
IN SOME $^{14}\text{N} + ^{59}\text{Co}$ SYSTEMS**

Department: **Physics**

Degree: **M.Sc** Convocation: **JUNE**

Year: **2012**

Permission is herewith granted to Addis Ababa University to circulate and to have copied for non-commercial purposes, at its discretion, the above title upon the request of individuals or institutions.

Signature of Author

THE AUTHOR RESERVES OTHER PUBLICATION RIGHTS, AND NEITHER THE THESIS NOR EXTENSIVE EXTRACTS FROM IT MAY BE PRINTED OR OTHERWISE REPRODUCED WITHOUT THE AUTHOR'S WRITTEN PERMISSION.

THE AUTHOR ATTESTS THAT PERMISSION HAS BEEN OBTAINED FOR THE USE OF ANY COPYRIGHTED MATERIAL APPEARING IN THIS THESIS (OTHER THAN BRIEF EXCERPTS REQUIRING ONLY PROPER ACKNOWLEDGMENT IN SCHOLARLY WRITING) AND THAT ALL SUCH USE IS CLEARLY ACKNOWLEDGED.

Table of contents

List of Tables	vi
List of Figures	vii
Abstract	viii
Acknowledgments	ix
1. Introduction	1
2. Nuclear Reaction Theories	3
2.1 Reaction Cross-section	4
2.2 Reaction Mechanisms.....	7
2.2.1 Direct Reactions	9
2.2.2 Compound Nucleus Reactions	10
2.2.3 Pre-equilibrium Reaction	13
2.3 Heavy ion Reactions.....	14
2.3.1 Complete Fusion of HI	15
2.3.2 Incomplete Fusion of HI	16
2.4 Nuclear Reactions and Models	18
2.4.1 Intra-nuclear Cascade Model	18
2.4.2 Harper-Miller-Berne Model	19
2.4.3 The Exciton Model	20
2.4.4 The Hybrid Model	23
2.4.5 Geometry Dependent Hybrid Model	24
3. Experimental Details	26
3.1 Experimental Method	26
3.2 Sample preparation.....	27
3.3 Experimental Errors	27
4. Result and Discussion	28
4.1 Computer Code Pace4	29
4.2 Computer Code Complet.....	30

4.3 Data Analysis.....	34
5. Conclusion	42
References	43

List of Tables

1. Table1: List of reactions identified along with the residues.....28
2. Table2: Experimentally measured Cross-sections for the residues.....28

List of Figures

1. Fig.2.1. Direct, pre-compound and compound nucleus contributions to a nuclear reaction.....	8
2. Fig. 2.2. Neutron emission spectrum showing contributions of different reaction mechanisms in nuclear reaction.....	8
3. Fig. 4.1 Excitation function for the $^{59}\text{Co}(^{14}\text{N},2n\alpha)^{67}\text{Ge}$ reaction used for studying the effect of value of k on theoretically calculated results.....	29
4. Fig. 4.2 Excitation function for the $^{59}\text{Co}(^{14}\text{N},np\alpha)^{67}\text{Ga}$ reaction used for studying the effect of exciton number n_0 on theoretically calculated results.....	31
5. Fig. 4.3 Excitation function for the $^{59}\text{Co}(^{14}\text{N},2p\alpha)^{67}\text{Zn}$ reaction used for studying the effect of COST parameter on theoretically calculated results.....	32
6. Fig. 4.4 Excitation function for the $^{59}\text{Co}(^{14}\text{N},2n2p)^{69}\text{Ge}$ reaction used for studying the effect of the value of 'k' on theoretically calculated results.....	33
7. Fig. 4.5 Excitation function for the $^{59}\text{Co}(^{14}\text{N},n\alpha)^{68}\text{Ge}$ reaction.....	34
8. Fig. 4.6 Excitation function for the $^{59}\text{Co}(^{14}\text{N},p\alpha)^{68}\text{Ga}$ reaction.....	35
9. Fig. 4.7 Excitation function for the $^{59}\text{Co}(^{14}\text{N},2n\alpha)^{67}\text{Ge}$ reaction.....	36
10. Fig. 4.8 Excitation function for the $^{59}\text{Co}(^{14}\text{N},np\alpha)^{67}\text{Ga}$ reaction.....	37
11. Fig. 4.9 Excitation function for the $^{59}\text{Co}(^{14}\text{N},2p\alpha)^{67}\text{Zn}$ reaction.....	38
12. Fig. 4.10 Excitation function for the $^{59}\text{Co}(^{14}\text{N},2n2p)^{69}\text{Ge}$ reaction.....	39
13. Fig. 4.11 Excitation function for the $^{59}\text{Co}(^{14}\text{N},n2\alpha)^{64}\text{Zn}$ reaction.....	40
14. Fig. 4.12 Excitation function for the $^{59}\text{Co}(^{14}\text{N},3np)^{69}\text{As}$ reaction.....	41

Abstract

The excitation functions for eight reactions produced in the interaction of $^{14}\text{N}+^{59}\text{Co}$ system measured in the energy range $\approx 32\text{-}56$ Mev and reported in the literature are compared with theoretical values calculated using the computer programs COMPLET and, a statistical model based Monte-Carlo simulation code PACE4. The effect of the variation of various parameters on calculated excitations functions have been studied. From this excitation functions study, the complete and incomplete fusion reactions in the light (medium) target nucleus could be studied. The present analysis shows that excitation functions are in good agreement with the theoretical predictions. It has been observed that complete fusion, incomplete fusion and pre-equilibrium emission processes play important roles in heavy ion reactions at these energies.

Acknowledgments

It is my pleasure to extend my deepest and sincere gratitude to my advisor Prof. A. K. Chaubey for his valuable assistance, guidance, supervision, patience with all my questions, suggestions and for providing necessary materials for the fulfillment of this thesis.

I am also thankful to Addis Ababa University (Department of Physics) for the financial support provided and for extending facilities for carrying out this thesis.

1. Introduction

Now a day the study of the interaction of two heavy ions has acquired a central place in nuclear physics research [1, 2]. This is possible with the availability of the accelerated beams of heavy ions. Recent studies show that there are different reaction mechanisms in heavy ion reactions at energies around the coulomb barrier to well above it. These reaction mechanisms have been discussed in recent papers [2].

The formation of compound nucleus is the dominant process at lower excitation energies. In compound nucleus formation reactions, the projectile is captured by the target nucleus and its energy is shared and re-shared among the nucleons of the compound nucleus until it reaches a state of statistical equilibrium. After a time much longer than the time required by the projectile to cross the nucleus, a nucleon or a group of nucleons near the surface may, by a statistical fluctuation, receive enough energy to escape, just as a molecule may evaporate from a heated drop of liquid.

At moderate excitation energies, however, there are indications that pre-equilibrium emission (where there is emission of a particle long before the attainment of statistical equilibrium) also contributes to the reaction processes.

Late experimental studies [2, 3] have shown that complete fusion and incomplete fusion reactions play important roles in heavy ion reactions. In the complete fusion reaction process of the projectile with the target, the projectile completely fuses with the target nucleus. In this case, the entire momentum of the projectile is transferred to the target nucleus. In the case of incomplete fusion reaction, only a part of the incident ion fuses with the target and the remaining part moves in the direction of the incident beam with almost the same velocity. In this case, the fraction of the momentum transferred depends on the mass of the fused fragment.

The main objective of this study is to study complete and incomplete reaction mechanisms in the light(medium) target nucleus. This is accomplished by the study of the excitation functions of the residues produced in the system $^{14}\text{N}+^{59}\text{Co}$.

This and other measurements [4] have shown the importance of complete and incomplete fusion as well as of pre-equilibrium emission processes in heavy ion reactions at energies around the coulomb barrier. The excitation functions for eight reactions produced in the $^{14}\text{N}+^{59}\text{Co}$ system have been measured in the energy range $\approx 32\text{-}56$ Mev to study complete fusion and incomplete fusion reactions in heavy ion reactions. Recently [4], it has been observed that the incomplete fusion becomes more and more dominant as the projectile energy increases.

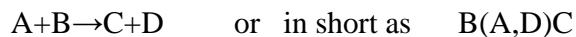
The present experimental values [5] are taken from experiments done using the S.Paulo Pelletron accelerator facility at Uni.de Sao Paulo, Sao Paulo, Brazil. The measured excitation functions are compared with theoretical calculations obtained using the computer programs pace4[2] and, complet[6] which evaluates the cross-sections for evaporation residues formed in the complete fusion reaction process of the projectile with the target without taking the incomplete fusion reaction process into account.

2. Nuclear Reaction Theories

Nuclear reaction is a process which occurs when the nucleons in the incident, or projectile, interact with the nucleons in the target. To do so a nucleon or a combination of nucleons (viz deuteron, alpha, heavy ion) must be very close to a nucleon or a nucleus so that these are under the influence of strong forces. In nuclear reaction there is a transfer of momentum (linear and angular), energy and nucleons, and some new systems are evolved and some particles are emitted. It is possible to define nuclear reaction as the interaction between nucleon and nucleon, nucleon and nucleus, and heavy ions and heavy ions.

The study of nuclear reactions is one important field of research to understand nuclear reaction mechanism and other nuclear structure properties. Most of the known nuclear reactions are produced by exposing different materials to a beam of accelerated nuclear particles. For nuclear reactions to occur the energy must be high enough to overcome the natural repulsion between the protons. This energy barrier is called the Coulomb barrier. If the energy is below the barrier, the reaction will bounce off each other.

Nuclear reaction [7] is generally represented as



Where B is the target, A is the projectile, C is the residual system and D is the emitted particle.

When a collision occurs between the incident particle and a target nucleus, either the beam particle scatters elastically having the target nucleus in its ground state or the target nucleus is internally excited and subsequently decays by emitting radiation or nucleons. A nuclear reaction is described by identifying the incident particle, target nucleus, and reaction products.

Nuclear reactions are subject to the conservation laws [1, 8]. These laws are the conservation of energy, momentum (linear and angular), total charge, mass number, spin, parity, baryon number, lepton number, etc.

The Q-value of any reaction is an important parameter that should be taken into consideration while studying nuclear reactions. It is defined as the energy released or absorbed in the reaction, given as

$$Q = (M_x + M_a - M_y - M_b) c^2 \quad (2.1)$$

Where M_x is the mass of the target, M_a is the mass of the projectile, M_y is mass of the residue, M_b is the mass of the emitted particle and c is the speed of light in vacuum.

There are different types of nuclear reactions [8]. Some of the reactions will be discussed below. Elastic scattering is a type of nuclear reaction where particle beam scattered and there is no appreciable energy loss by the projectile. No excitation of nucleus takes place. In this type of reaction small energy loss is required to conserve the momentum.

Inelastic scattering is other type of nuclear reaction. In this type of nuclear reactions, there is an appreciable energy loss and the target nucleus is in the excited state after reaction.

Radiative capture is also other type of nuclear reaction where the projectile is captured by the target nucleus such that the energy of excitation is not very high. Here there may be high energy γ -ray emission.

Disintegration is a nuclear reaction type whereby there is emission of different particles because depending upon the energy of the projectile the system may disintegrate. Here different residual systems are possible with different combination of emitted particles, and also low energy γ -rays may be associated.

Nuclear fusion and fission reactions are other types of nuclear reactions. In fusion reaction there is a combination of two nuclei to form a more massive nucleus where as in fission reaction there is a disintegration of a heavy nucleus into different fragments.

2.1 Reaction Cross-section

Reaction cross-section [7] is the most important quantity in nuclear reaction study. The reaction cross-section is a measure of the probability for a particular reaction to occur. Since interactions in a nuclear reaction take place with individual target nuclei independently of each other, it is useful to refer to the probability of a nuclear reaction to one target nucleus.

To define the reaction cross-section, assume that in a given experiment a thin slab of target material is struck by mono energetic beam consisting of I particles per unit time distributed uniformly over an area A . If nuclear reaction produces N particles per unit time, we can pretend that with each target nucleus there is associated an area σ which is perpendicular to the incident beam such that if the center of a bombarding particle strikes inside of σ , there is a hit and a reaction is produced; and if the center of the bombarding particles misses σ , no reaction is produced.

So the quantity σ is defined as cross-section and it gives a measure of the reaction probability per target nucleus. It is a fictitious area, which need not be related to the cross-sectional area (πR^2) of the struck nucleus.

It is also possible to describe the reaction probability by the ratio $\frac{N}{I}$, but this quantity depends on the target density as well as its thickness Δx , where as σ is associated with an individual target nucleus.

The probability that any one bombarding particle has a hit is equal to $\frac{N}{I}$ and is also equal to the projected total cross-section of all target nuclei lying within the area A , as seen along the beam direction, divided by A . If there are n target nuclei per unit volume in the target material, $nA\Delta x$, such nuclei are within reach of any bombarding particle in the beam. Each target nucleus has an associated cross-section σ so that $\frac{N}{I} = \frac{nA\Delta x\sigma}{A}$

Using this relation we can define cross-section by writing

$$\sigma = \frac{N}{(I/A)(nA\Delta x)} \quad (2.2)$$

The cross-section has a dimension of area and measured in a unit of cm^2 or barn, where

1barn= 10^{-24}cm^2 . Experimentally cross-section is measured by the ratio

$$\sigma = \frac{\text{number of reaction particles emitted}}{(\text{number of beam particles per unit area})(\text{number of target nuclei within the beam})}$$

The impact parameter is an important parameter in nuclear reactions to take place, as stated earlier, and it has a connection with the reaction cross-section-the probability for nuclear reaction to take place. To see this connection, consider the projectile beam as particle wave. There will be interaction of beam with target, from classical considerations, when the impact parameter of beam is less than the nuclear radius i.e., if $b \leq R$ interaction takes place and if $b > R$ no interaction is taking place.

Angular momentum is given as $\mathbf{p} \times \mathbf{b}$ or $\mathbf{p}b$. But from quantum mechanics, angular momentum is quantized and is given as $\ell\hbar$, where $\ell=0, 1, 2, \dots$. From this relation we can write angular momentum as $pb=\ell\hbar$ or the impact parameter $b=\ell\hbar/p$ or $b=\lambda\ell$. Where $\lambda=\hbar/p$ is the reduced de Broglie wave length. This clearly shows that the idea of quantization of angular momentum leads to the quantization of impact parameter.

We can imagine particles of beam moving with having different quantized value of impact parameter. One can divide the particles of beam in different zones having different impact parameters. Particles moving in the central zone having $\ell=0$ and impact parameter $b \leq \lambda$. In the next zone particles of impact parameter of b value $\lambda < b < 2\lambda$ having $\ell=1$ are moving. In the next zone particles having $\ell=2$ and impact parameter $2\lambda < b < 3\lambda$ are moving. In this way particles moving in ℓ^{th} zone will have impact parameter in between $\ell\lambda$ and $(\ell+1)\lambda$. Geometrical area of ℓ^{th} zone will be

$$\pi[(\ell+1)\lambda]^2 - \pi(\ell\lambda)^2 = \pi\lambda^2(2\ell+1)$$

So the reaction cross-section, $\sigma_{r,\ell}$ is given as

$$\sigma_{r,\ell} = \pi\lambda^2(2\ell+1) \text{ or}$$

$$\sigma_r = \sum_l \pi\lambda^2(2l+1) = \pi\lambda^2 \sum_{l=0}^{lm} (2l+1)$$

$$\sigma_r = \pi\lambda^2 \sum_{l=0}^{lm} (2l+1) \quad (2.3)$$

2.2 Reaction Mechanisms

In nuclear reaction [1], there are three mechanisms of nuclear reaction. These are direct reaction, compound nucleus reaction and pre-equilibrium reaction. The direct reaction takes place in the time the projectile takes to traverse the target nucleus ($\sim 10^{-22}$ s). In this reaction, the projectile may interact with a nucleon; a group of nucleons or with the whole nucleus and emission takes place immediately.

The compound nucleus reaction takes place when the projectile is captured by the target nucleus. In this reaction, the energy and momentum of the projectile is shared and re-shared among the nucleons of the compound nucleus until it reaches a state of statistical equilibrium. This transfer of energy and momentum takes so much time ($\sim 10^{-15}$ s) that the incoming projectile becomes part of the system because there is a thorough mixing of all the nucleons energy.

The pre-equilibrium reaction is a reaction mechanism where a particle is emitted neither immediately after the interaction of the projectile with a nucleon or with a group of nucleons of the target nucleus, as in a direct reaction, nor after a long time by the statistical decay of the compound nucleus. The projectile may share its energy among a small number of nucleons which may further interact with other nucleons, and this cascade of nucleon-nucleon interactions through which the energy of the incident particle is progressively shared among the target nucleons, a particle may be emitted long before the attainment of statistical equilibrium.

All these reactions are subject to the conservation laws of energy, momentum, mass number, spin, total charge, parity, lepton number, baryon number, etc. The relative importance of these three reaction mechanisms depends on the type of interacting particles and their relative energy.

In these different types of reaction mechanisms, after the first interactions, the nucleon may leave the nucleus immediately by a direct reaction or it may interact with a nucleon in the nucleus and start a cascade of nucleon-nucleon interaction from which pre-equilibrium emission may occur. During this cascade, the energy is shared among an increasing number of nucleons until eventually the compound nucleus is formed. The compound nucleus may decay into the elastic or any of the reaction channels that are allowed energetically. The shape elastic and compound elastic processes combine to give the measured elastic scattering cross-section. In a similar way the direct, pre-equilibrium and compound nucleus processes combine to give the inelastic cross-sections and all

the other non-elastic reactions. This shows the connection between the different reaction mechanisms.

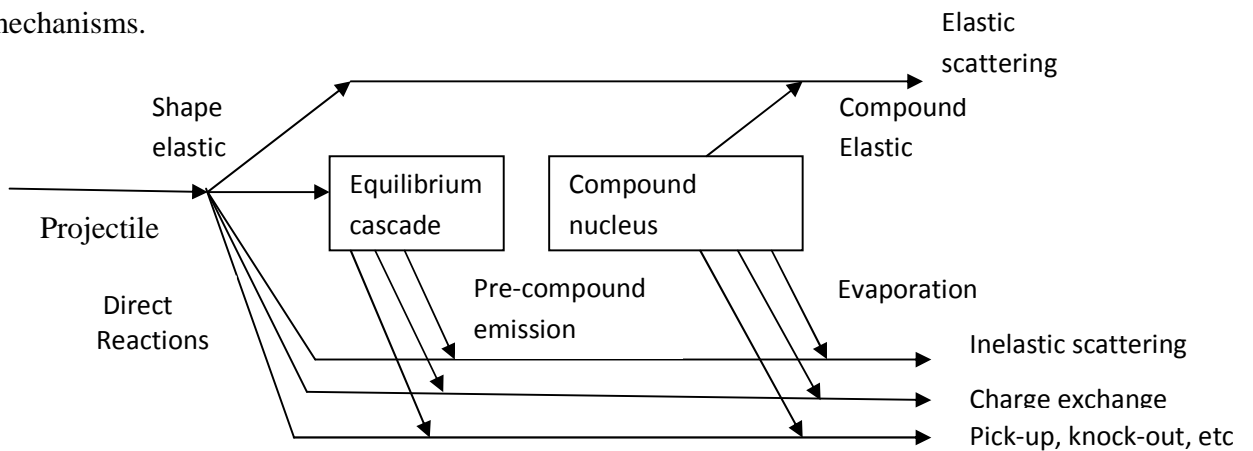


Fig. 2.1 Direct, pre-compound and compound nucleus contributions to a nuclear reaction.

All the above mentioned reaction mechanisms may contribute to a given reaction and an experiment may focus on one contribution or the other. To show this, consider the elastic scattering of a nucleon or a proton by a nucleus. At low energies, neutrons and protons interact very differently. Protons are repelled by the electrostatic field of the nucleus and are scattered elastically with a cross-section given by Rutherford's formula. This is a direct reaction. Low energy neutrons may be scattered by the nuclear field (this is potential scattering, or shape elastic scattering, a direct process) or may be captured to form the compound nucleus and then emitted with the same energy. This is compound elastic scattering, which is strongly affected by the structure of the compound nucleus.

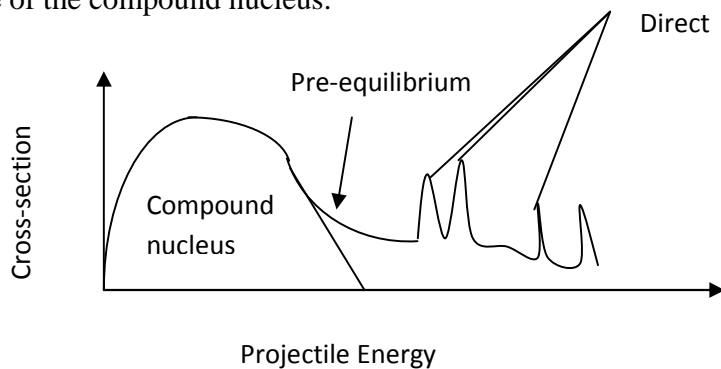


Fig. 2.2 Neutron emission spectrum showing contributions of different reaction mechanisms in nuclear reaction.

2.2.1 Direct Reactions

A direct reaction [1] occurs when the projectile interacts primarily with the nucleons in the surface of the target nucleus. The interaction is with one or two nucleons. Energy and momentum transfer is very small and the transfer is to only few nucleons, and emission of the particle most probably is in the direction of motion of the projectile.

The main characteristics of direct reactions are: first the emission of much larger number of high energy particles than expected on the basis of evaporation model. Second, the angular distribution of emitted particles shows a forward peaking. This is may be because the direct reaction takes place with surface nucleons. The third main characteristic of direct reaction is a monotonic change of cross-section with energy, no resonances are observed. Direct reactions take place, generally, at higher energies.

There are a number of reactions categorized under the direct reaction. The simplest direct reaction is elastic scattering, which leaves the target nucleus in its ground state. Inelastic scattering occurs when a projectile interacts with a target nucleus and gives it some of its energy, raising it to an excited state. Measurement of the loss of energy gives the energy of the excited state.

At low incident energies the target nucleus can be excited purely by the coulomb excitation and is appreciable only for highly charged projectiles-heavy ions. At higher energies the excitation is due to the nuclear interaction between the projectile and target modified by the presence of the coulomb field. By inelastic scattering, mainly, it is collective states that are strongly excited. This shows that the projectile interacts with the target nucleus as a whole, not just with one of its constituent nucleon. This is a collective excitation and may be described as a coherent sum of many individual particle-hole excitations.

Charge-exchange reaction is other type of direct reaction. In this reaction both energy and charge are transferred between the projectile and the target nucleus. Charge-exchange reactions show the importance of isospin in nuclear reactions. These reactions are particularly interesting because only the charge-exchange isospin-dependent terms in the effective interaction contribute to the cross-section. If the reaction goes to the isobaric analogue state of the target nucleus the reaction is particularly simple as only the isospin vectors are flipped. Such reactions are very similar to elastic scattering, and are sometimes referred to as quasi-elastic scattering.

The other reaction under the direct reaction is transfer reaction. In this reaction one or more nucleons are transferred from the projectile to the target-stripping or from the target to the projectile-pick up reactions.

As the energy of the projectile increases, it becomes likely that more than one particle is emitted. The simplest examples are the break-up of a composite projectile into its constituents and the knock-out of a nucleon or group of nucleons from the target nucleus. At low projectile energies, the break-up is due to the coulomb field of the target nucleus, and as the energy increases the nuclear field also contributes. Coulomb break-up is more pronounced for heavy target nuclei. Break-up reactions can have the target in its ground state, or raise it to an excited state; these processes referred to as elastic and inelastic break-up. In a knock-out reaction the incident particle is small compared with the inter nucleon separation in the nucleus, and the projectile energy is much higher than the binding energy of the struck nucleus.

2.2.2 Compound Nucleus Reactions

A compound nucleus reaction [1] is an extreme example of a multistep reaction in which the detailed complexity of the successive steps is lost. In compound nucleus reaction a transfer of energy and momentum takes so much time that the compound nucleus formed forgets the history of formation. If the same compound nucleus is formed by different projectile interactions. It cannot remember the mechanism of its formation.

A compound nucleus state is excited, and gives resonances when the energy brought in by the projectile, plus the capture Q-value coincides with energy of one of its states. These states are excited one by one as the energy increases, and each corresponds to resonance.

It is difficult to give a rigorous description of the process of formation of the compound nucleus. It is a good approximation to assume that, in the sequence of nucleon-nucleon interactions, all the states corresponding to the various configurations are excited with equal probability. When eventually the long-lived compound nucleus is created, all the possible states corresponding to a given set of quantum numbers E, J, M, π , from the single-particle to the complex many-particle states, are equally likely. The compound nucleus is then in statistical equilibrium since the probability of occurrence of a given configuration is simply proportional to its statistical weight.

In compound nucleus reactions, after a time much longer than the time required by the projectile to cross the nucleus, a nucleon or a group of nucleons near the surface may, by statistical fluctuation, receive enough energy to escape, just as a molecule may evaporate from a heated drop of liquid. This statistical process favors the evaporation of the particles with energy near the smallest possible energy, which in the case of charged particle is the height of the coulomb potential at the nuclear surface, the coulomb barrier. If the excitation energy of the compound nucleus is high enough, several particles may evaporated in sequence and the process continues until the energy of the nucleus is below the threshold for the particle emission, and then the nucleus emits γ -rays until it reaches the ground state.

The decay of the compound nucleus is independent of the way it is formed. Its decay will depend only on its quantum mechanical parameter-energy of excitation and momentum. Decay of any excited state depends upon the width of decaying state i.e. $\Gamma = \frac{\hbar}{\tau}$, where τ is mean life of decaying state. The decay probability of compound nucleus is given as $G_c(\beta) = \frac{\Gamma_\beta}{\Gamma}$. The probability of formation of compound nucleus by α -channel is $\sigma(\alpha, \beta) = \sigma_c(\alpha) \frac{\Gamma_\beta}{\Gamma}$, where α is incoming channel while β is outgoing channel.

The Weisskopf-Ewing theory [1] is the best theory for describing compound nucleus reactions. At low incident energies the compound nucleus states are excited individually each produces a resonance in the cross-section that may be described by the Breit-Wigner theory. As the incident energy increases compound nucleus states of higher energy are excited and these are closer together and of increasing width. Eventually they overlap and it is no longer possible to identify the individual resonances. The cross-section then fluctuates.

This fluctuating behavior is due to the interference of the reaction amplitudes corresponding to the excitation of each of the overlapping states which vanish in the energy average of the cross-section since these amplitudes are complex functions with random modules and phase. The energy average of the cross-sections thus shows weak energy dependence and it is predicable by the theory. To do this, consider a reaction that proceeds from the initial channel c through the compound nucleus to the final channel c' .

The hypothesis of the independence of formation and decay of the compound nucleus then gives for the cross-section $\sigma_{cc'} \approx \sigma_{CN}(c) \frac{\Gamma_{c'}}{\Gamma}$, where $\sigma_{CN}(c)$ is the cross-section of the compound nucleus and $\Gamma_{c'}$ and Γ are respectively the energy-averaged width for the decay of the compound nucleus in channel c' and the energy-averaged total width.

Using the reciprocity theorem, which relates the cross-section $\sigma_{cc'}$ to the cross-section for the time reversal process $c'c$, we get

$$g_c k_c^2 \sigma_{cc'} = g_{c'} k_{c'}^2 \sigma_{c'c} \quad (2.4)$$

where $g_c = 2i_c + 1$ and $g_{c'} = 2i_{c'} + 1$ are the statistical weights of the initial and final channels, i_c and $i_{c'}$ the spin of the projectile and the ejectile, and k_c and $k_{c'}$ their wave numbers. This gives

$g_c k_c^2 \sigma_{CN}(c) \Gamma_{c'} = g_{c'} k_{c'}^2 \sigma_{CN}(c') \Gamma_c$ or equivalently

$$\frac{\Gamma_c}{g_c k_c^2 \sigma_{CN}(c)} = \frac{\Gamma_{c'}}{g_{c'} k_{c'}^2 \sigma_{CN}(c')} \quad (2.5)$$

Since the channels c and c' are chosen arbitrarily, this relation holds for all possible channels. So

$\Gamma_c \propto g_c k_c^2 \sigma_{CN}(c)$. Since the total width is obtained by summing the $\Gamma_{c'}$'s over all open channels $\Gamma = \sum_c \Gamma_c$, the cross-section $\sigma_{cc'}$ becomes

$$\sigma_{cc'} = \sigma_{CN}(c) \frac{g_{c'} k_{c'}^2 \sigma_{CN}(c')}{\sum_c g_c k_c^2 \sigma_{CN}(c)} \quad (2.6)$$

Ejectiles with energy in the range $\epsilon_{c'}$ to $\epsilon_{c'} + d\epsilon_{c'}$, have the residual nucleus with energy in the range $U_{c'}$ to $U_{c'} + dU_{c'}$, where $U_{c'} = E_{CN} - B_{c'} - \epsilon_{c'}$, and E_{CN} and $B_{c'}$ are respectively compound nucleus energy and the binding energy of the ejectile in the compound nucleus.

Introducing the density of levels of the nucleus $w(u_{c'})$ the above equation becomes

$$\sigma_{cc'} d\epsilon_{c'} = \sigma_{CN}(c) \frac{g_{c'} k_{c'}^2 \sigma_{CN}(c') w(u_{c'}) du_{c'}}{\sum_c \int_0^{E_c^{\max}} g_c k_c^2 \sigma_{CN}(c) w(u_c) du_c} \quad \text{or since } k^2 = 2m\epsilon,$$

$$\sigma_{cc'}(\epsilon_{c'}) d\epsilon_{c'} = \sigma_{CN}(c) \frac{(2i_{c'} + 1) \mu_{c'} \sigma_{CN}(c') w(u_{c'}) du_{c'}}{\sum_c \int_0^{E_c^{\max}} (2i_c + 1) \mu_c \sigma_{CN}(c) w(u_c) du_c} \quad (2.7)$$

where μ_c is the reduced mass of the ejectile c . This is the Weisskopf-Ewing formula for the angle integrated cross-sections.

To a good approximation, the level density $w(u) \propto \exp\left(\frac{u}{T}\right)$, so the ejectile spectrum given by the Weisskopf-Ewing theory is Maxwellian. It rises rapidly above the threshold energy, attains a maximum and then falls exponentially.

From the detailed balance principle which in addition to the invariance for the reversal leading to the reciprocity theorem implies the existence of a long-lived compound nucleus state. This principle states that two systems a and b , with state densities ρ_a and ρ_b , are in statistical equilibrium when the depletion of the states of the system a by transition to b equals their increase by the time reversal process $b \rightarrow a$.

If $w_{ab} = \frac{\Gamma_{ab}}{h}$ is the decay rate (probability per unit time) for transitions from a to b and $w_{ba} = \frac{\Gamma_{ba}}{h}$ is the decay rate for the reverse process, this equality occurs when $\rho_a \Gamma_{ab} = \rho_b \Gamma_{ba}$.

The Weisskopf-Ewing theory provides a simple way of estimating the energy variation, at low incident energies, of the cross-section of all available final channels in a particular reaction.

2.2.3 Pre-equilibrium Reaction

Pre-equilibrium reaction [1] is neither direct nor compound nucleus reaction. In this type of reactions particles are emitted after the first stage of a nuclear interaction (direct reaction) but long before the attainment of statistical equilibrium (compound nucleus formation). Their time scale is intermediate between the very fast direct reactions and the relatively slow compound nucleus formation.

In pre-equilibrium reactions, the emission of particles from the excited target nucleus is neither by statistical decay of compound nucleus nor by the prompt emission after collision. In these reactions, the projectile shares its energy among a small number of nucleons in the target; the struck nucleons initiate a cascade of reactions with the target, at the course of which a particle can be emitted before the compound nucleus was reached a state of statistical equilibrium.

The energy of the projectile is shared among the nucleons of the target by a cascade of nucleon-nucleon interactions that excites particle-hole state of increasing complexity. A pre-equilibrium reaction corresponds to emission of an unbound particle from one of these particle-hole states when the composite nucleus is not yet equilibrated.

Most pre-equilibrium reactions take place at energies high enough for it to be no longer possible to resolve the individual final state. The cross-sections are those of reactions to a continuum of final states, and the absence of fluctuations in these continuum spectra shows that to a high degree of accuracy one may assume that there are no interference effects so that pre-equilibrium cross-sections can be evaluated by adding incoherently the contributions from each stage of the nucleon-nucleon interaction cascade. The total cross-section for pre-equilibrium emission is then the sum of the cross-sections for emission from each stage of the cascade.

2.3 Heavy ion Reactions

The study of two heavy ions reaction is a subject of growing interest in nuclear physics [1, 9, 10]. Particles (projectiles) heavier than α -particles are considered as heavy particles. Almost every element can be produced in ionized form and an accelerated beam of any heavy ion can be produced. The complex nature of the projectile makes it possible that a number of new reactions occur, and also when the projectile fuses with the target nucleus creating a compound nucleus one has to consider the special features of heavy ion reaction due to the large angular momentum carried in by the projectile.

At low energies two heavy ions interact only through their coulomb field, and can scatter elastically or in-elastically with coulomb excitation. Nuclear interactions can only take place if the two ion energy E_{cm} in their center of mass system is high enough to overcome the coulomb barrier, and then the associated wavelength $\lambda = \frac{h}{\sqrt{2ME_{cm}}}$ is much less than the nuclear dimensions.

In heavy ion reactions there may be a transfer of huge mass or large number of nucleons—from a single nucleon transfer to a large number of nucleons transfer may take place. There is also very large energy and momentum transfer in heavy ion reactions. In these reactions, highly excited states with large angular momentum transfer (high spin states) are there. Due to large amount of

mass transfer and also in the decay (after reaction), there are emission of several types of systems- light particles, nucleons and also heavy fragments (elements).

It has been observed that at energies just above the coulomb barrier, the dominant reaction mechanism in heavy ion reactions are complete and incomplete fusion. In the complete fusion reactions, the incident ion completely fuses with the target nucleus, forming an excited compound system, from which particles and/or γ -ray may be emitted. In the case of incomplete fusion, the projectile is assumed to break-up into fragments, one of which fuses with the target nucleus while the rest of it moves in the forward direction with almost the same velocity as that of incident ion. The excited system formed as a result of the fusion of one of the fragments of the incident ion may also undergo de-excitation by the emission of particles and/or γ -rays.

2.3.1 Complete Fusion of HI

Heavy ion complete fusion reaction [1, 2, 3, 9] is a reaction where there is an entire momentum transfer from projectile to the target nucleus takes place. In this reaction, a fully equilibrated excited compound nucleus of pre-determined charge, mass and angular momentum is formed. Heavy ion fusion reactions have been extensively studied because they offer possibility of producing nuclei with high excitation energy and high spin thus allowing study of nuclear matter in conditions which are not easily formed in other reactions. Fusion reactions have also been used to try produce super-heavy nuclei and to produce proton rich nuclei very far from the stability line.

There are important features of fusion reactions. For light projectiles and low incident energies the fusion cross-section may be a considerable fraction of the reaction cross-section. The second important feature is, with increasing charge of the interacting ions the fusion probability falls abruptly. The other feature of fusion reaction is the fusion cross-section at first increases linearly with $\frac{1}{E_{cm}}$, reaches a maximum and thereafter decrease linearly with $\frac{1}{E_{cm}}$. The detailed energy dependence of the fusion cross-section may differ quite considerably for different interacting ions forming the compound nucleus. In general, the fusion cross-section varies quite smoothly with the energy, but in the case of light systems it may show quite large oscillations.

When two heavy ions fuse, they form a compound nucleus which is far from statistical equilibrium since a large fraction of its energy is in form of an orderly collective translational

motion of the nucleons of the projectile and the target. This orderly motion transforms into chaotic thermal motion through a cascade of nucleon-nucleon interactions during the thermalization of the compound nucleus. This takes some time and before reaching thermal equilibrium, nucleons or clusters of which still have energy considerably higher than their equilibrium thermal energy may be emitted into the continuum. These pre-equilibrium emissions must be taken into account to reproduce the multiplicity and the spectra of the ejectiles measured in heavy ion fusion reactions.

The ejectiles emitted in a fusion reaction at rather low incident energies are detected in coincidence with the residue, of mass near to the compound nucleus, emitted at a very forward angle with a velocity about equal to that expected for a complete momentum transfer.

At higher incident energies this is no longer valid since the excitation energy of the compound nucleus is very high and it emits, before reaching statistical equilibrium, so many particles that the velocity of the residue is considerably less.

The excitation functions of several heavy ion fusion reactions depart from what is expected for purely evaporative contributions. Starting from bombarding energies only slightly above the coulomb barrier acting between the two interacting ions and seem to be satisfactorily reproduced only if emission of pre-equilibrium nucleons is taken into account. Some calculations [1] suggest that with increasing bombarding energy an increasing fraction of the excitation energy is dissipated by emitting pre-equilibrium particles (about 50% at an energy about 30MeV/nucleon), greatly reducing the probability of forming very excited equilibrated nuclei.

2.3.2 Incomplete Fusion of HI

Incomplete fusion reaction [1, 2, 3, 9, 10] is a reaction where fractional mass, charge and momentum of the projectile are transferred to the target nucleus due to the prompt emission of projectile fragment(s) in the forward direction with almost projectile velocity.

There are various binary break-up processes. Elastic break-up with immediate emission of both fragments originating from the break-up and no excitation of the target, which may be released by coincidence experiments, inelastic break-up in which both fragments come out after the interaction, but one of them after having interacted with the target nucleus, which further de-excites with emission either of particles or γ -rays, and break-up fusion or incomplete fusion in

which only one of the fragments come out (the spectator fragment) while the other (the participant fragment) is absorbed by the target nucleus which may be considerably excited.

In elastic and inelastic break-up reactions both fragments are emitted where as in break-up fusion or incomplete fusion processes only one of the fragments come out while the other is absorbed by the target nucleus. The importance of this process is revealed by the study of excitation functions of reactions induced by complex projectile.

Incomplete fusion reaction has also been observed in the interaction of light ions [1, 11] such as ^{12}C , ^{14}N and ^{16}O with heavy targets. These ions may break-up preferentially into α -type fragments (for instance, in the case of Nitrogen it may break-up in to ^{10}B and α -particle or ^6Li and two α -particles) where one of which further fuses with the target nucleus.

The contribution of the incomplete fusion cross-sections may be separated from the complete fusion in several ways. The first evidence for such phenomena was found by measuring the angular correlation of fission fragments. Fusion reactions lead to emission of fragments at relative less angles and are the dominant contribution at all the energies considered, but, with a probability increasing with energy, almost back-to-back fragment emissions are also observed. This may only occur if, as in incomplete fusion, a momentum considerably smaller than that of the projectile is transferred to the fissioning compound nucleus.

Further experiments [1] measured the incomplete fusion cross-section by detecting the spectator fragment in coincidence with the γ -lines of the incomplete fusion residue or by measuring (by activation techniques) the recoil ranges and the angular distribution of the incomplete fusion residues. These last experiments are based on the consideration that a compound nucleus formed in an incomplete fusion reaction has, respectively, a smaller linear momentum and a larger recoil angle than a compound nucleus formed in a complete fusion process.

As a consequence the residues also have a smaller range and a larger recoil angle and both effects contribute to reduce the projection of their recoil range in the beam direction. Thus, if a residue is formed both in fusion and in an incomplete fusion, the two contributions may be separated by looking at their forward recoil range distribution. Even more effective in separating the two contributions may be angular distribution measurement. Residues of fusion reaction, especially at not too high incident energies where emission of intermediate mass fragment is quite improbable,

are concentrated in a forward direction along the beam direction. Those formed in incomplete fusion processes recoil to angles appreciably different from zero.

2.4 Nuclear Reactions and Models

Many recent [12] heavy-ion experiments have provided evidence for non-equilibrium particle emission. An appropriate reaction model is necessary to interpret the physical message that the experimental observations convey. If the model has the important parameters properly included, the interpretation of the observations may lead to understanding. Suitable models for heavy-ion pre-compound decay phenomena may provide the necessary bridge in understanding the transition between low energy compound nucleus reactions and the fragmentation reactions of higher incident energies.

Among the several semi-classical models which have been proposed in reproducing a large body of experimental data are the Hybrid and Geometry Dependent Hybrid models. They have been reasonably successful in reproducing a broad range of experimental data. This was accomplished with several choices of parameter options.

Recently quantum mechanical theories of pre-equilibrium emission have been proposed. These quantum mechanical models [12] provide, in principle, way of calculating the cross-sections of pre-equilibrium processes without the uncertainties of the semi-classical approximations. These models are in the early stage of application, at the present. Even for light heavy-ion particle α , the quantum mechanical treatment of the initial particle-target interaction become very complicated.

2.4.1 Intra-nuclear Cascade Model

The Intra-nuclear cascade model [12] was first proposed by Serber and first implemented to explain the interactions of high energy neutrons with complex nuclei. In INC model the projectile enters the target nucleus with a given parameter “b”. The projectile interacts with the target nucleons after travelling a certain distance inside the target nucleus, and excites it above the Fermi Sea. Each scattered particle then travel through the nucleus interacting with the other nucleons.

The INC model traces the individual nucleon trajectories in three-dimensional geometry. The trajectories of all excited particle are followed until some arbitrary energy significantly above the mean equilibrium value has been attained by the nucleon. Particles reaching the nuclear surface

with sufficient energy are assumed to be emitted. When all particles of a given cascade have been traced, the total energy of the residual nuclei, its identity, and the energies and angles of the emitted particles are shared, and a new cascade with new impact parameter is calculated with help of such an approach, the time evolution of the reaction can be generated but after few collisions the actual calculations becomes too much complicated. The INC model is a realistic model but in general, the model prediction is not satisfactorily at backward angles and is some forward angles also.

2.4.2 Harp-Miller-Berne Model

In Harp-Miller-Berne model [12], the nuclear single particle states are classified according to their energies in groups or “bins” whose size ΔE is chosen to be of some convenient dimension. In the calculations, the fractional occupation of each bin is taken as function of time. This model calculates the occupation probability of an average state in i^{th} bin as a function of time using Fermi gas distribution. At the initiation of the reaction, at the time τ_0 all the levels below the Fermi energy are filled up (as the target is in ground state), and the projectile is in an excited state. This gives the fractional occupation probability at time $\tau=\tau_0$. Two-body interactions then lead to a redistribution of probabilities.

After calculating the relative probabilities of scattering into and out of each bin and the emission from bins above the particle binding energies, populations of all bins are changed accordingly. The calculation is repeated until a steady state configuration is reached. At each time during the equilibrium process the energy spectrum of emitted nucleons are calculated and a net spectrum obtained.

Later by Harp and Miller in HMB model, a minor modification is suggested. They considered the nucleus to be composed of independent proton and neutron Fermi gases. Therefore, the proton and neutron occupation numbers for the single particle states of these gases completely specifies the internal configuration of the nucleus at any time. Further, it is also assumed that the mechanism for the equilibrium of the gases takes place through binary nucleon-nucleon collisions. Correspondingly a new set of master equation is obtained, the solution of which gives the proton and neutron occupation numbers.

2.4.3 The Exciton Model

The Exciton Model [1, 12] is first introduced by Griffin in 1996 and later modified by many workers. In the Exciton model, the compound nucleus states are characterized by the number of excited particles and holes (the excitons) at any stage of the nucleon-nucleon cascade. In this model the equilibration between target and projectile is achieved by the succession of nucleon-nucleon interactions. An excited nucleus is considered as a gas of quasi-particles i.e., particle-hole degree of freedom is included.

The initial configuration is fixed by the nature of the projectile. For instance in case of a nucleon-induced reaction, it is a two-particle-one hole configuration due to the interaction of the incident nucleon with a nucleon of the target which is excited from a state below to a state above the Fermi energy. Additional two-body interactions give rise to a sequence of states characterized by increasing exciton numbers, eventually leading to a fully equilibrated residual nucleus.

Restriction to two-body interactions leads to the following selection rules concerning the possible variation of the number of particles, p , hole, h , and excitons, $n=p+h$, in the course of the cascade of interactions:

$$\Delta p=0, \pm 1 \quad \Delta h=0, \pm 1 \quad \Delta n=0, \pm 2$$

The states which are excited in the course of this interaction cascade are very unstable. In exciton model intermediate states play significant role in dealing with PE processes.

Single particles densities are often used to calculate the exciton level densities, assuming the nucleus to be distinguishable Fermi gas with equidistance level. The transition rates are proportional to level density of the final accessible states (Fermi Golden rule). Ericson's level density result, at a given exciton number, n with excitation energy E_{ex} is

$$\rho_n(E_{ex}) = \frac{g(gE_{ex})^{p+h-1}}{p!h!(p+h-1)!} \quad (2.8)$$

in this equation g is the one-particle state density, E_{ex} is the excitation energy, and p and h are the number of excited particles and holes respectively. William gave expression for the particle-hole density by considering the effect of the Pauli exclusive principle in the uniform spacing model as

$$\rho_n(E_{ex}) = \frac{g(gE_{ex} - A(p,h))^{p+h-1}}{p!h!(p+h-1)!} \quad (2.9)$$

$$\text{where } A(p,h) = \frac{1}{2}(p^2 + h^2 + p - h) - \frac{1}{2}h.$$

The probability of decay from an n exciton state $\rho_n(E_{ex})$ is defined as the ratio of the emission rate from n to the rates of all transitions (including emission) from n . If $\lambda_c^n(\varepsilon)$ be the emission rate with energy ε (in the interval $d\varepsilon$) from the n exciton state and $\lambda_{\pm,0}^n$ the probabilities for the transitions corresponding to the charge of the exciton number $\Delta n = \pm 2, 0$

$$\rho_n(\varepsilon) = \frac{\lambda_c^n(\varepsilon)}{\lambda_+^n + \lambda_-^n + \lambda_0^n + \int d\varepsilon \lambda_c^n(\varepsilon)} \quad (2.10)$$

The exciton model assume that (1) at each stage of the cascade all the states with the same configuration and the same total energy are equi-probable, and (2) at each stage of the cascade all the processes which may occur are also equi-probable.

The first assumption implies that partitioning of energy occurs with equal probability. Hence emission rates are summed over all ε in the denominator to obtain $\rho_n(\varepsilon)$. The emission rates as obtained from the principle of detailed balance is given by

$$\lambda_c^n(\varepsilon) = \frac{(2s+1)}{h} \left[\frac{\rho_{n'}(u)}{\rho_n(E_{ex})} \right] m \varepsilon \sigma_{inv}(\varepsilon) \quad (2.11)$$

here s and m are the intrinsic spin and reduced mass of the ejectile, n' is the exciton number after emission of ejectile with v nucleons: $n' = n - v$, u is the residual excitation energy given by

$$u = E_{ex} - B - \varepsilon, \text{ with } B \text{ the ejectile separation energy, } \sigma_{inv} \text{ is the inverse cross-section.}$$

Using Fermi's Golden rule the transition rates are defined as

$$\lambda_+^n = \frac{2\pi}{h} [M_+]^2 \rho_{n+2}, \quad \Delta n = +2$$

$$\lambda_-^n = \frac{2\pi}{h} [M_-]^2 \rho_{n-2}, \quad \Delta n = -2$$

$$\lambda_0^n = \frac{2\pi}{h} [M_0]^2 \rho_n, \quad \Delta n = 0$$

Here $[M_{0,\pm}]$ are the matrix elements of the corresponding transitions. ρ_{n+2}, ρ_{n-2} and ρ_n are the density of states available in the $n+2$, $n-2$, and n exciton states after $\Delta n=2, -2$ and 0 transitions. The estimation of the transition matrix element $[M_{0,\pm}]$ proves to be one of the most crucial points in the model. A common estimation is to assume $M_+ = M_- = M_0 = M$. Using the assumption and the consequent restriction imposed on, the density of final states, the transition states were given by Williams as

$$\begin{aligned}\lambda_+ &= \frac{2\pi}{\hbar} [M]^2 \frac{g^3 E^2}{2(n+1)} & \Delta n = +2 \\ \lambda_0 &= \frac{2\pi}{\hbar} [M]^2 g^2 E \frac{3n-2}{4} & \Delta n = 0 \\ \lambda_- &= \frac{2\pi}{\hbar} [M]^2 g \rho(n-2), & \Delta n = -2, \quad \text{where } E \text{ is the excitation energy of the system.}\end{aligned}$$

Compound nuclear equilibration is attained when the rate of creation of p-h pairs approximately equals the annihilation rates of such pair, so that the exciton number $n=n'$ remains unchanged.

Assuming that $\lambda_{n+2} = \lambda_{n-2} = \lambda_0$ at equilibrium i.e., $n=n'$ it follows

$$n' \cong \sqrt{2gE} \quad (2.12)$$

At low excitation energy, it is reasonable to assume energy independent matrix element, while at higher excitation energies, energy dependent matrix elements are used. The analysis of a large body of data indicates that a mass and energy dependence of the average square matrix for nucleon-nucleon interaction given by Kalback's estimate, according to which $[M]^2$ has the following mass number A and energy E_{ex} dependent

$$[M]^2 = kA^{-3} E_{ex}^{-1} \quad (2.13)$$

where k is an adjustable parameter ranging from 95-700 Mev.

2.4.4 The Hybrid Model

A decade ago predictions of pre-equilibrium decay in heavy ion reactions were made by using the hybrid model [12]. The H model for pre-equilibrium decay is formulated as

$$\sigma_{\text{pec}}(\varepsilon) = \sigma_{\text{abs}} \sum_{\substack{n=n_0 \\ \Delta n=+2}}^{n'} D_n p_v^n(\varepsilon) \quad (2.14)$$

where $p_v^n(\varepsilon)$ is the emission probability of v with energy between ε and $\varepsilon+d\varepsilon$ from the n exciton states. The pre-equilibrium decay probability is given by

$$p_v(\varepsilon)d\varepsilon = \sum_{\substack{n=n_0 \\ \Delta n=+2}}^{n'} \left[\frac{n X_n N_n(\varepsilon, u)}{N_n(\varepsilon)} \right] g d\varepsilon \times \left[\frac{\lambda_c^n(\varepsilon)}{\lambda_c(\varepsilon) + \lambda_+(\varepsilon)} \right] D_n \quad (2.15)$$

where $p_v(\varepsilon)d\varepsilon$ is the number of particles of the type v emitted into the unbounded continuum with channel energy between ε and $\varepsilon+d\varepsilon$.

The quantity in the first bracket of eq(2.15) represents the number of particles to be found (per Mev) at a given energy ε (with respect to continuum) for all scattering processes leading to an “ n ” exciton configuration. The nucleon-nucleon scattering energy partition function $N_n(\varepsilon)$ is identical to the exciton state density $\rho_n(E_{\text{ex}})$ and $N_n(\varepsilon)$ represent number of combinations with which n exciton may share E_{ex} . The second set of bracket of eq(2.15) represents the fraction of the v type particles at energy ε which should undergo emission into the continuum, rather than making an inter-nucleon transition. The D_n represents the average fraction of the initial population surviving to the exciton number being treated.

In the hybrid model the probability of energy partitioning in the exciton state, n is borrowed from the HMB model. The HMB model determine the nucleon-nucleon interaction rate $\lambda_+(\varepsilon)$ from the free nucleon-nucleon scattering cross-sections to avoid the uncertainties associated with the values of $[M]^2$. The H model also calculates $\lambda_+(\varepsilon)$ from the nucleon-nucleon scattering cross-sections. But instead of experimental cross-sections it uses either Kikuchi-Kawai calculations or the empirical expression for the two-body interaction rate given by Blann by simplifying the detailed Kikuchi-Kawai calculations. The empirical expression is as follows

$$\lambda_+^n = [1.4 * 10^{21} (\varepsilon + B_{\text{sp}}) - 6 * 10^{18} (\varepsilon + d_\varepsilon + B_{\text{sp}})^2] \text{k}^{-1} \quad (2.16)$$

where ε is the particle energy outside the nucleus i.e., ejectile energy and B_{sp} its separation energy k is an adjustable constant. When $k=1$ equation (2.16) reproduces the Kikuchi-Kawai interaction rates.

2.4.5 Geometry Dependent Hybrid Model

Geometry dependent hybrid (GDH) model [12] has been reasonably successful in reproducing a broad range of data. This was accomplished with several choices of parameter options. The geometry dependent hybrid model is a variant of the HM in which the nuclear geometry effects are considered. GDH model takes into account the reduced matter density and hence also the shallow potential. In this way the diffused surface properties sampled by higher impact parameter were incorporated into the pre-compound decay formalism in the geometry dependent hybrid model.

The differential emission spectrum is given in the GDH model as

$$\frac{D\delta_v(\varepsilon)}{d\varepsilon} = \pi\tilde{\lambda}^2 \sum_{l=0}^{\infty} (2l+1) T_l P_v(l, \varepsilon) \quad (2.17)$$

Where $P_v(l, \varepsilon)d\varepsilon$ is as for $P_v(\varepsilon)d\varepsilon$, but evaluated for the l^{th} partial wave. T_l is the transmission coefficient for the l^{th} partial wave, and $\tilde{\lambda}$ is the reduced de-Broglie wave length. The GDH model and codes using this model employed a Fermi density distribution,

$$d(R_l) = d_s \left[\frac{\exp(R_l - c)}{0.55 \text{fm}} + 1 \right]^{-1}, \quad (2.18)$$

where d_s is the saturation density of nuclear matter and c is the charge radius with $c=1.07A^{1/3}\text{fm}$, taken from electron scattering result. The charge radius c of equation above has been replaced in the present parameterization by a value characteristic of matter (rather than charge) radius based on the droplet model work of Myers plus an adhoc projectile range parameter $\tilde{\lambda}$,

$$c = 1.18A^{1/3} \left[1 - \frac{1}{(1.18A^{1/3})^2} \right] + \tilde{\lambda} \quad (2.19)$$

Here the average nuclear density is determined by interaction and averaging of eq(2.18) between $R=0$ and $R=c+2.75\text{fm}$. The Fermi energy, ε_f has been taken as 40MeV for saturation density, and is assumed to vary as the average density to the two-third power. The value of ε_f so evaluated is used in defining the single particle level density ‘‘g’’ for all calculations, H and GDH models, as

this should be a property of the average potential. The single particle level densities have been defined by

$$g_n = \frac{N}{20} \left[\frac{\varepsilon_f + B_{Sp} + \varepsilon}{\varepsilon_f} \right]^{1/2} \quad (2.20)$$

$$g_p = \frac{Z}{20} \left[\frac{\varepsilon_f + B_{Sp} + \varepsilon}{\varepsilon_f} \right]^{1/2} \quad (2.21)$$

3. Experimental Details

The experimental [5] excitation functions used in this study were obtained using the facility S.Paulo Pelletron accelerator. The experiment was conducted at Uni.de Sao Paulo, Sao Paulo, Brazil. It is not possible to conduct the experiment here in Ethiopia since there is no such facility available. So there is no experimental result available for comparison.

3.1 Experimental Method

The typical experimental arrangement for the study of nuclear reactions is an accelerator producing a collimated mono-energetic beam, a target containing the nuclei being studied and detectors of the emerging particles (ejectiles).

The quantity one measures most frequently is the energy distribution of particles emitted at a given angle, the so called double differential spectra, which may be integrated over the angles to provide the angle integrated spectra.

The excitation function is also one of the quantities one measures most frequently. Excitation function is the angle integrated cross-section for a given reaction as a function of the projectile energy. Excitation function is very easily measured when the reaction produces a radioactive residue, by detecting the activity induced in the target and/or a set of absorbers downstream from the target. This gives the number of residues which are produced from which one deduce the total cross-section for the reaction concerned.

In this study, the fusion and transfer cross-sections were determined by the in-beam and off-beam gamma ray spectroscopy methods, which allow the simultaneous measurement of fusion, transfer channels and inelastic scattering cross-sections. The transfer cross-sections determined are a lower limit of the total transfer yield, since they corresponds to transfer processes leading to the excited states from which gamma transitions are detected.

Experimentally, the cross-section $\sigma_r(E)$ at a given energy E for different reactions was determined using the expression [2],

$$\sigma_r(E) = \frac{c\lambda e^{\lambda t}}{No\xi\phi\theta Ge(1-e^{-\lambda t})(1-e^{-\lambda t})} \quad (3.1)$$

Where $c\lambda$ is activity of the isotope produced in the reaction, t_1 is the time lapse between the end of irradiation and the start of the counting, λ the decay constant of the isotope produced, N_0 is the number of target nuclei irradiated in the time interval t_1 , ϕ is the incident flux, θ is the branching ratio of identified γ -ray, and G_e is the geometry dependent efficiency of the detector for a particular energy E .

The quantity ξ is the correction for self absorption of the γ -ray with absorption coefficient μ for the sample of thickness d , and it is given as

$$\xi = \frac{(1 - e^{-\mu d})}{\mu d} \quad (3.2)$$

3.2 Sample preparation

In the sample, the target consisted of pure metallic Cobalt, with thickness in the range 200-400 $\mu\text{-g}/\text{cm}^2$, evaporated on Pb backings thick enough to stop the beam, in order to avoid Doppler shifts of the gamma-lines. For each bombarding energy a different target was used, avoiding undesirable contributions to the spectra coming from the decay of previous irradiations.

3.3 Experimental Errors

There were experimental errors in the value of the fusion cross-sections due to (1) statistical errors in the determination of the gamma yields, (2) systematic errors due to the target thickness, absolute efficiency and faraday-cup or thick target calculation for coulomb excitation and (3) errors from the contaminants corrections. The overall error is in the range from 8% at higher energies to almost 20% at very low energies.

4. Result and Discussion

The excitation functions for the reactions $^{59}\text{Co}(^{14}\text{N},n\alpha)^{68}\text{Ge}$, $^{59}\text{Co}(^{14}\text{N},p\alpha)^{68}\text{Ga}$, $^{59}\text{Co}(^{14}\text{N},2n\alpha)^{67}\text{Ge}$, $^{59}\text{Co}(^{14}\text{N},np\alpha)^{67}\text{Ga}$, $^{59}\text{Co}(^{14}\text{N},2p\alpha)^{67}\text{Zn}$, $^{59}\text{Co}(^{14}\text{N},2n2p)^{69}\text{Ge}$, $^{59}\text{Co}(^{14}\text{N},n2\alpha)^{64}\text{Zn}$, and $^{59}\text{Co}(^{14}\text{N},3np)^{69}\text{As}$ have been measured in the beam energy range $\approx 32\text{-}56$ Mev. A list of reactions and residues detected are given in table 1 where as the experimental cross-sections of the residues are given in table 2.

Table1: List of reactions identified along with the residues

Reaction	Residue
$^{59}\text{Co}(^{14}\text{N},n\alpha)$	$^{68}_{32}\text{Ge}$
$^{59}\text{Co}(^{14}\text{N},p\alpha)$	$^{68}_{31}\text{Ga}$
$^{59}\text{Co}(^{14}\text{N},2n\alpha)$	$^{67}_{32}\text{Ge}$
$^{59}\text{Co}(^{14}\text{N},np\alpha)$	$^{67}_{31}\text{Ga}$
$^{59}\text{Co}(^{14}\text{N},2p\alpha)$	$^{67}_{30}\text{Zn}$
$^{59}\text{Co}(^{14}\text{N},2n2p)$	$^{69}_{32}\text{Ge}$
$^{59}\text{Co}(^{14}\text{N},n2\alpha)$	$^{64}_{30}\text{Zn}$
$^{59}\text{Co}(^{14}\text{N},3np)$	$^{69}_{33}\text{As}$

Table2: Experimentally measured Cross-sections for the residues

Lab Energy(Mev)	Cross-section for residues(mb)							
	$^{68}_{32}\text{Ge}$	$^{68}_{31}\text{Ga}$	$^{67}_{32}\text{Ge}$	$^{67}_{31}\text{Ga}$	$^{67}_{30}\text{Zn}$	$^{69}_{32}\text{Ge}$	$^{64}_{30}\text{Zn}$	$^{69}_{33}\text{As}$
32	4.2	1.8	-	-	4.5	-	-	-
34	7.5	5.4	-	4	9.2	-	4	-
36.5	82	14.2	-	16.6	12.9	-	8.7	1.2
40	22	17.6	3.2	45.3	20.8	1.2	12.9	3.1
45	35	21.3	12.5	82.3	27.8	11.2	17.7	4.2
48	38.9	36.1	21.8	108	37.7	33.6	31.3	6.9
51	34	34.4	34.1	138	51	72.9	37.9	7.3
56	27.4	39.5	46.8	174	96	129	51.8	15

The measured excitation functions have been compared with theoretical predictions based on computer codes complet and pace4. To the best of our knowledge these measurements have been done for the first time and hence no data is available for comparison. The details of these calculations and the parameters used are discussed below.

4.1 Computer Code Pace4

The pace4 code [2] is based on a statistical approach. In this program the de-excitation of the compound nucleus is followed by a Monte-Carlo procedure. The angular momentum projections are calculated at each stage of de-excitation, which enables the de-excitation of the angular distribution of the emitted particles. The level density parameter is an important parameter which may be varied to match the experimental data. The effect of variation in the level density parameter constant 'k' on calculated excitation functions for the $^{59}\text{Co}(^{14}\text{N}, 2n\alpha)^{67}\text{Ge}$ reaction is shown in Fig.4.1. As can be observed from this figure, a value of 'k'=8 satisfactorily reproduces the measured excitation functions.

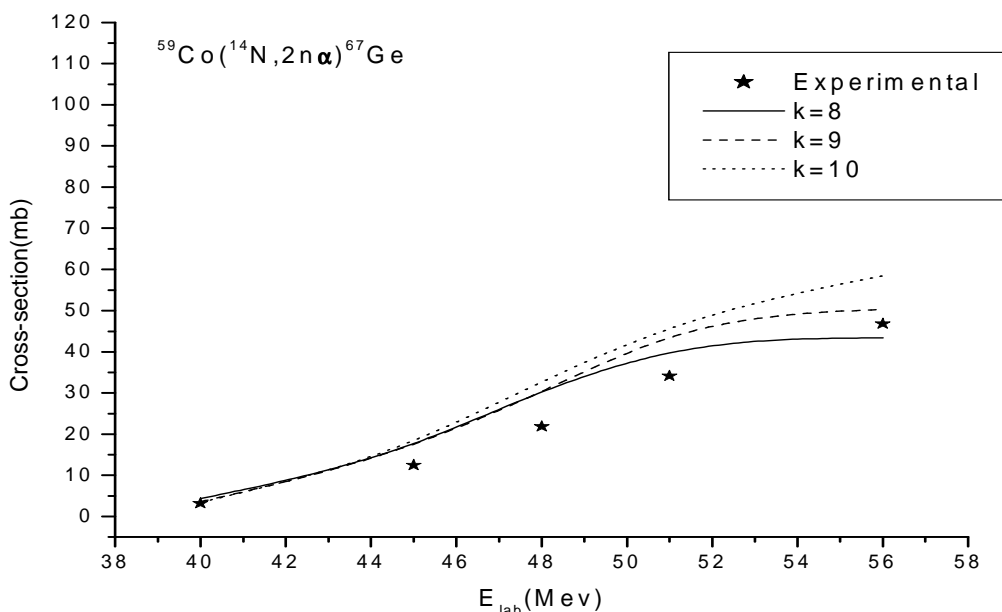


Fig. 4.1 Excitation function for the $^{59}\text{Co}(^{14}\text{N}, 2n\alpha)^{67}\text{Ge}$ reaction used for studying the effect of the value of k on theoretically calculated results.

4.2 Computer Code Complet

The complet code [6], originally, has been developed out of the code overlaid Alice by M.Blann. In this code, while some standard routines remained particularly unchanged (like FISROT, LYMASS, PUNCH, PLT, PARAP, OVER1, OVER2 and TLJ) others have been substantially modified (like MAIN, SHAFT, NUCMFP, etc) or are completely new (like INDEX, PARDEN, TRAPRO, ANGULAR, etc).

The complet code includes damping of fission widths above a critical temperature, rotating liquid drop fission barriers and rotational energies due to Seirk included for $j_{cal}=0$. Still M&S or Exp. Masses are used as before. The code complet includes pre-equilibrium neutron, proton and alpha emission up to two particles as well as evaporation of neutron, proton, alpha, deuterons, tritons and hellions.

The complet code is based on the Weisskopf-Ewing model [1, 2] for compound nucleus calculations and the Hybrid model for simulating pre-equilibrium emission. The code assumes equi-partition of energy among the initially excited particles and holes. The code uses Gove mass tables or the Myers Swiatecki/Lysekil mass formula. The option that substitutes Gove's table for Myers Swiatecki/Lysekil mass formula including shell corrections was used. In order to calculate inverse cross-sections, the optical model subroutine with the parameters of Becchetti and Greenless was employed.

The important parameters of the complet code are the level density parameter a , initial exciton number n_0 , and the mean free path multiplier COST. The first parameter greatly affects the equilibrium component, through the level densities. The level density parameter 'a' is calculated using the relation $a=A/k$, where A is the mass number of the compound system and k is a constant which may be varied to match the experimental data. The parameter n_0 and COST greatly govern the pre-equilibrium component.

The initial exciton number n_0 decides the complexity of the initial configuration. A smaller value of n_0 , means that the initial state is less complex and hence far from the equilibrium. As such, a larger pre-equilibrium contribution is expected. On the other hand, a large value of n_0 , means that the system is nearer to the equilibrium stage and therefore, small pre-equilibrium contribution is likely.

In order to see the effect of variation of n_0 on calculated excitation functions, calculations were done by varying n_0 from 14 to 16. As a representative case, these calculations for $^{59}\text{Co}(^{14}\text{N},n\text{p}\alpha)^{67}\text{Ga}$ channel are shown in Fig. 4.2. It may be seen from this figure that a value of $n_0=14$ is best suited for the present experimental data, even though the effect is not as such significant as shown, clearly, in the figure. The value of $n_0=14$ may be justified assuming that the projectile ^{14}N breaks up in the nuclear field of the target nucleus creating 14 excitons.

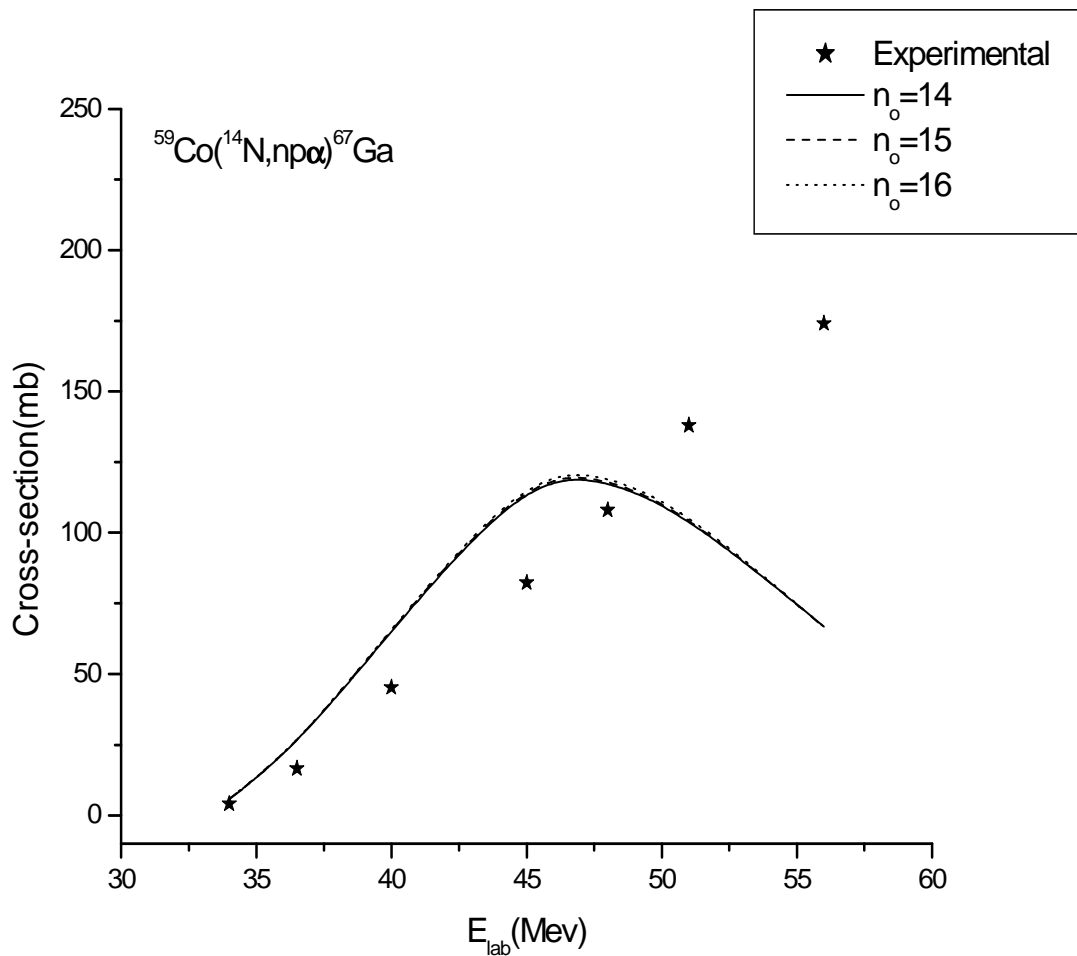


Fig.4.2 Excitation function for the $^{59}\text{Co}(^{14}\text{N},n\text{p}\alpha)^{67}\text{Ga}$ reaction used for studying the effect of excitation number n_0 on theoretically calculated results.

The parameter COST, which is used to adjust the mean free path for two-body residual interactions inside the nuclear matter, is varied from 1 to 4 and its effects on excitation function for $^{59}\text{Co}(^{14}\text{N},2p\alpha)^{67}\text{Zn}$ reaction is shown in Fig. 4.3, as a representative case. The value of COST=1 is best suited for the present experimental data.

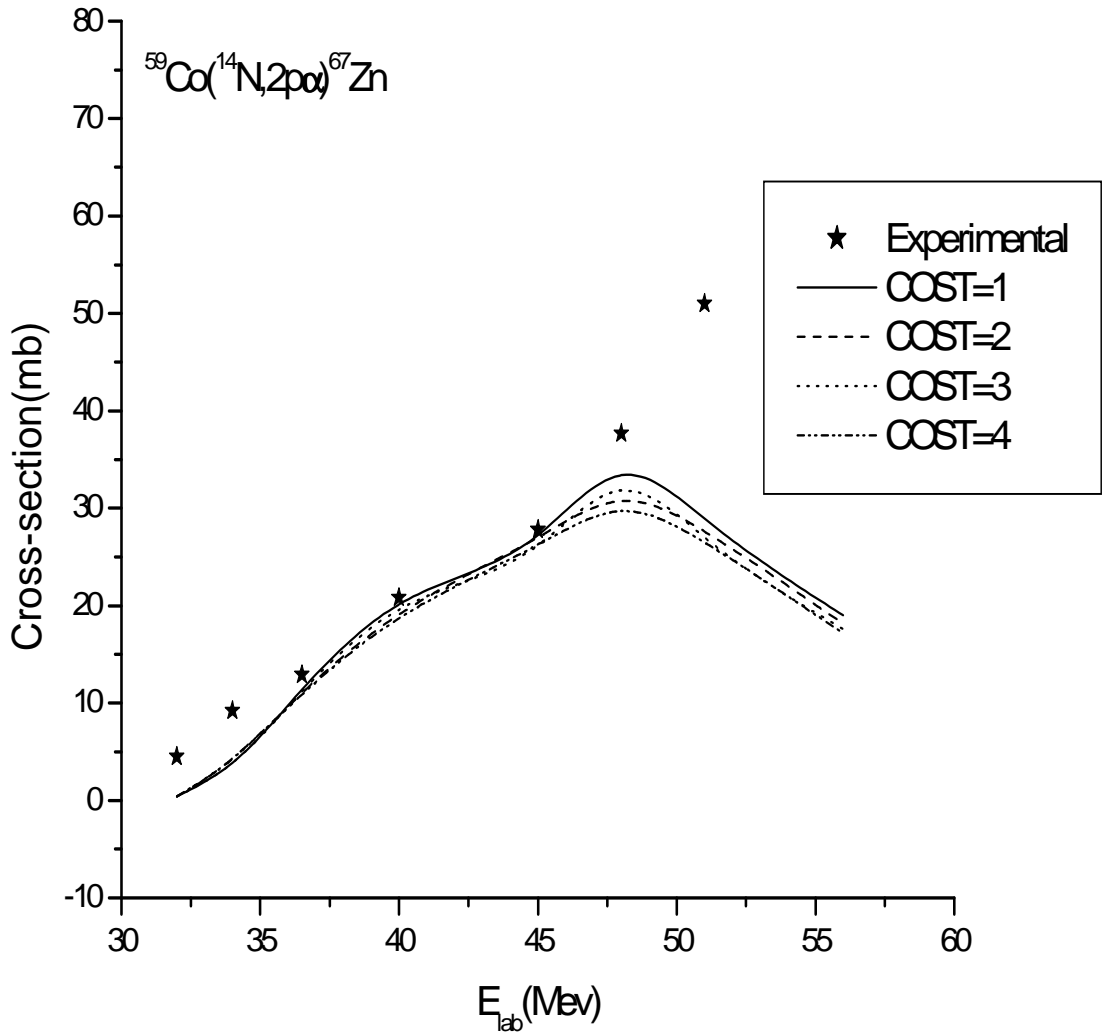


Fig.4.3 Excitation function for the $^{59}\text{Co}(^{14}\text{N},2p\alpha)^{67}\text{Zn}$ reaction used for studying the effect of COST parameter on theoretically calculated results.

The effect of the variation of 'k' on the calculated excitation functions was also studied. The value of 'k' was varied from 8 to 10. As a typical example, the calculated excitation functions for the $^{59}\text{Co}(^{14}\text{N},2n2p)^{69}\text{Ge}$ reaction for different values of 'k' are shown in the Fig. 4.4. As can be seen from this figure, and in general also, the present experimental data is best reproduced with a value of 'k'=8.

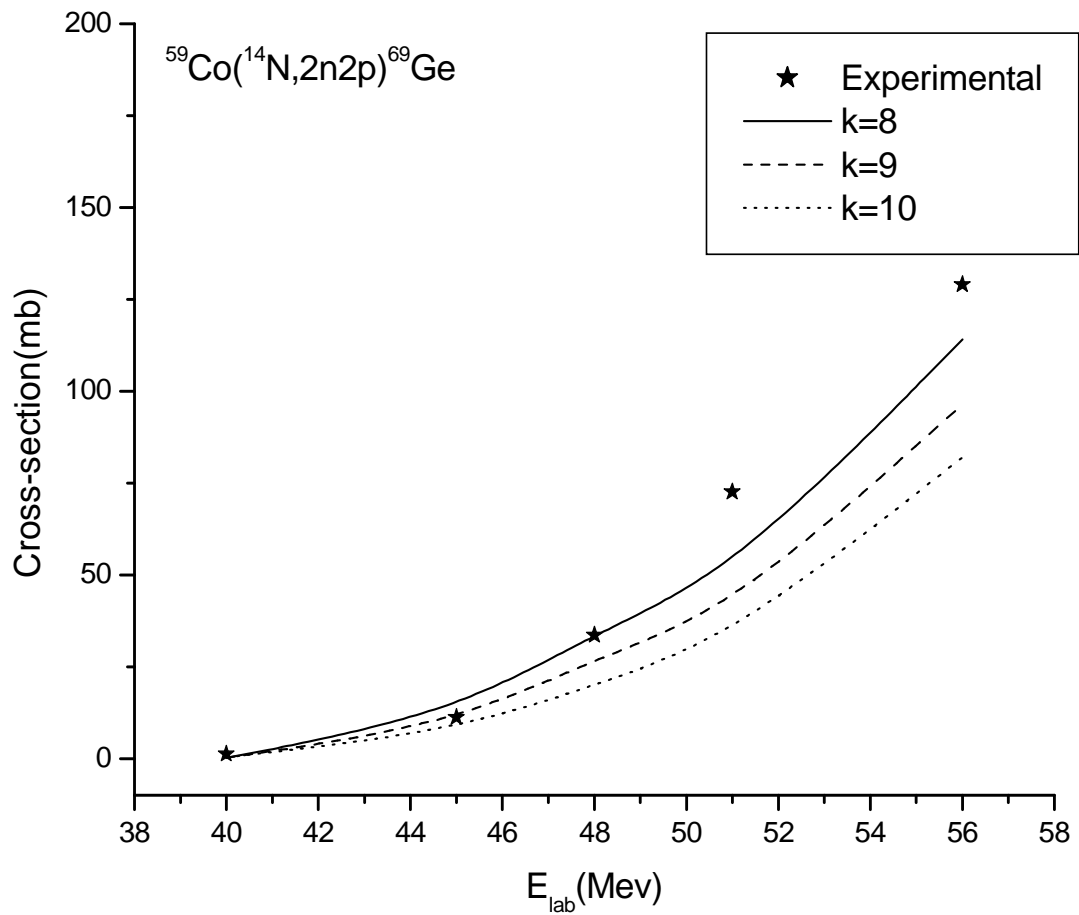


Fig.4.4 Excitation function for the $^{59}\text{Co}(^{14}\text{N},2n2p)^{69}\text{Ge}$ reaction used for studying the effect of the value of 'k' on theoretically calculated results.

In general, it may be pointed out that a set of 'k'=8, $n_0=14$ with COST=1 gives a satisfactory reproduction of the magnitude of the experimental data.

4.3 Data Analysis

Here experimentally measured results are compared with theoretical obtained calculations. The theoretical calculations are based on the computer codes Pace4 and Complet which are discussed before. So the data analyses of the results are based on these computer codes.

For the $^{59}\text{Co}(^{14}\text{N},n\alpha)^{68}\text{Ge}$ reaction, as shown in Fig. 4.5, the pace4 result is slightly in good agreement with the experimental result at lower energies where as the calculations from complet code, both for compound nucleus formation and pre-equilibrium emissions, are negligible as compared to experimental results at lower as well as higher energies. The experimental result is larger than the theoretical calculations at higher energies. This difference in the experimental and theoretical calculations may be due the contributions coming from incomplete fusion. In this reaction it may be assumed that the projectile (^{14}N) break-up into α and ^{10}B . The ^{10}B fragment fuses with the target (^{59}Co) forming the excited state $^{69}\text{As}^*$ while the rest fragment moves in the forward direction almost with the same velocity. The excited state $^{69}\text{As}^*$ may then emits one neutron, during thermalization, leaving behind the residual nucleus ^{68}Ge .

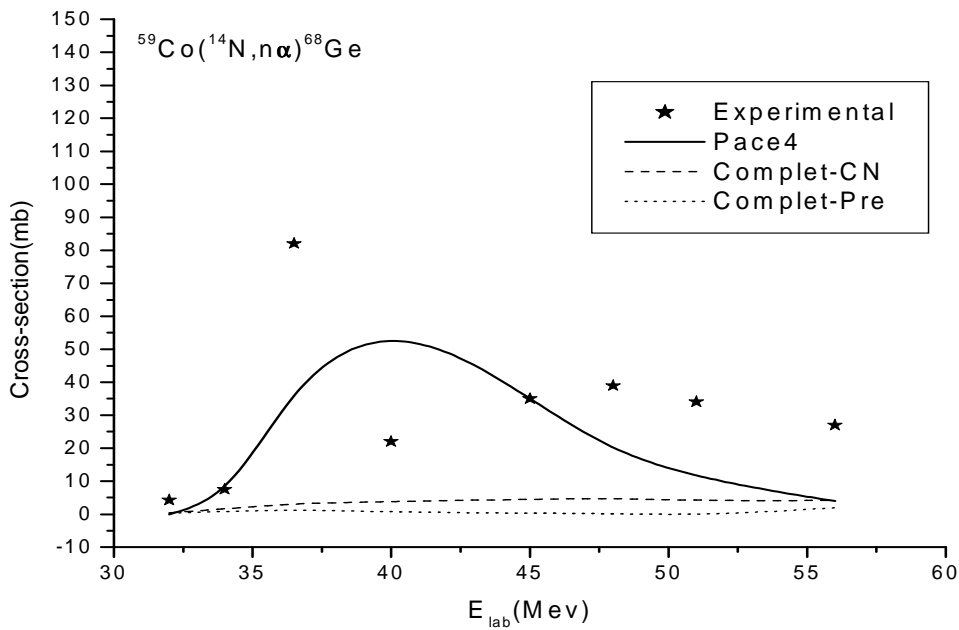


Fig.4.5 Excitation function for the $^{59}\text{Co}(^{14}\text{N},n\alpha)^{68}\text{Ge}$ reaction

In the $^{59}\text{Co}(^{14}\text{N},p\alpha)^{68}\text{Ga}$ reaction, as can be clearly seen in Fig. 4.6, the pace4 and complet codes give good results which agree with the experimental results at lower energies. As the energy gets increasing, there is an agreement only between theoretically calculated complet-CN results and the experimentally obtained results. So for this reaction, complete fusion of the projectile with the target takes place. The production of ^{68}Ga leads to the sequential decay of alpha particle and proton in the de-excitation of the compound nucleus formed ($^{73}\text{Se}^*$) during the complete fusion of ^{14}N with ^{59}Co . There is a negligible projectile break-up in to α and ^{10}B .

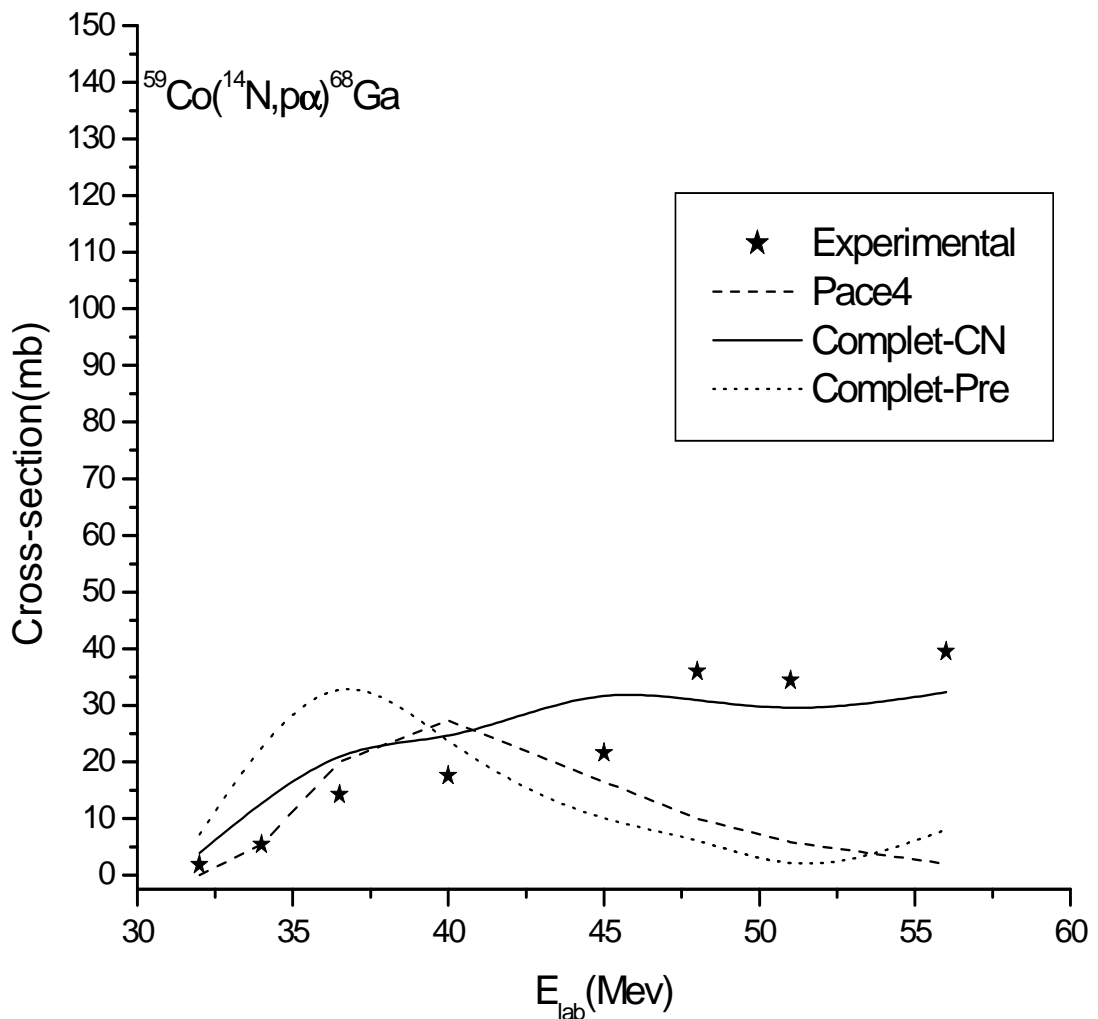


Fig.4.6 Excitation function for the $^{59}\text{Co}(^{14}\text{N},p\alpha)^{68}\text{Ga}$ reaction

In the $^{59}\text{Co}(^{14}\text{N},2n\alpha)^{67}\text{Ge}$ reaction, the pace4 result is in good agreement with experimentally measured excitation functions whereas the complete results are negligible, especially at higher energies. Complete fusion of the projectile with the target takes place. The production of ^{67}Ge leads to the sequential decay of alpha particle and two neutrons in the de-excitation of the compound nucleus formed during the complete fusion of ^{14}N with ^{59}Co . There is a negligible projectile break-up into α and ^{10}B . Complete fusion reaction is dominant and the small disagreement may be due to statistical uncertainties in the pace4 calculations.

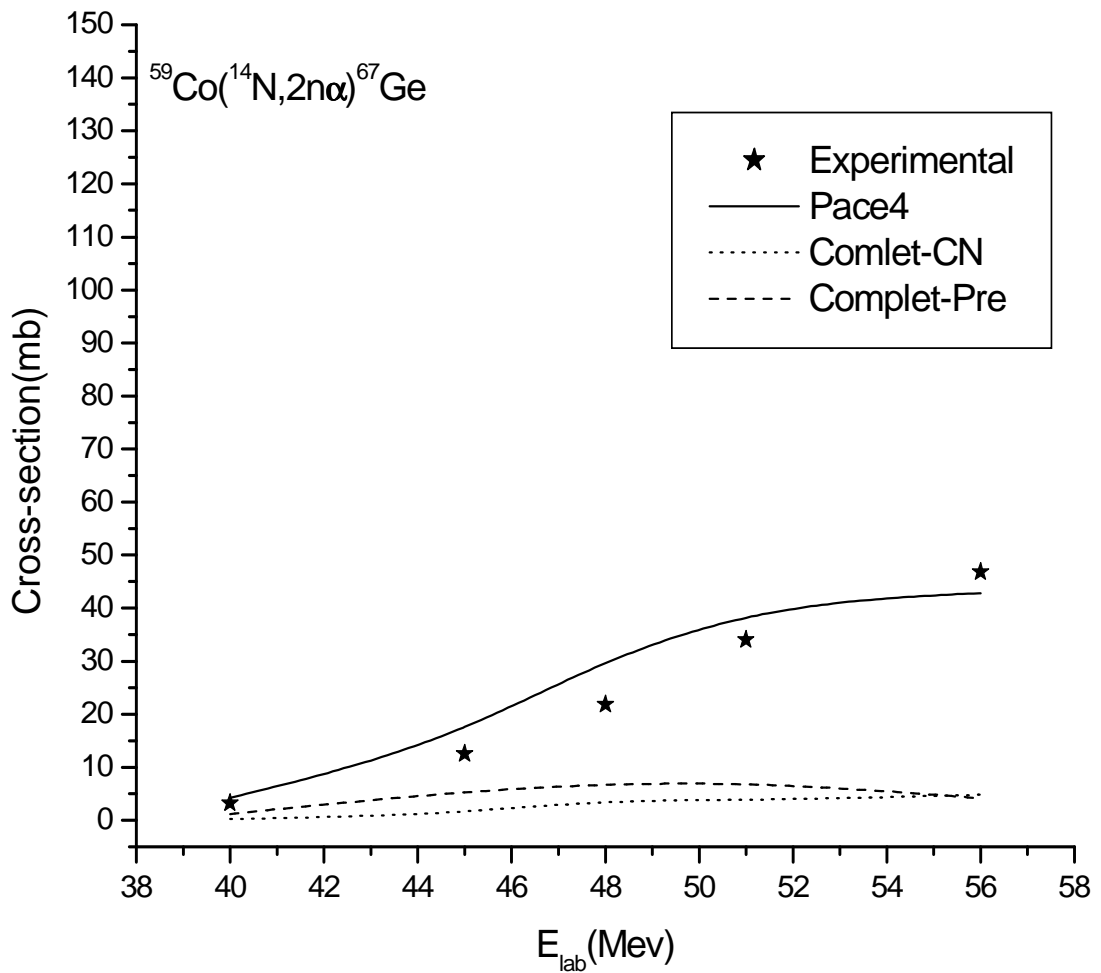


Fig.4.7 Excitation function for the $^{59}\text{Co}(^{14}\text{N},2n\alpha)^{67}\text{Ge}$ reaction

For the $^{59}\text{Co}(^{14}\text{N},n\text{p}\alpha)^{67}\text{Ga}$ reaction, the theoretically calculated results using complet and pace4 are slightly closer to the experimental results, at lower energies. At higher energies there arises a disagreement between theoretical calculations and experimentally measured values, as can be seen from the figure. For this reaction, it is possible to assume the break-up of the projectile into α and ^{10}B . The ^{10}B fuses with the target forming the excited state $^{69}\text{As}^*$, which emits one neutron and one proton, during the thermalization, leaving behind the residual nucleus ^{67}Ga . So the disagreement between the experimental and theoretical calculations could be inferred to the contributions coming from the incomplete fusion reaction.

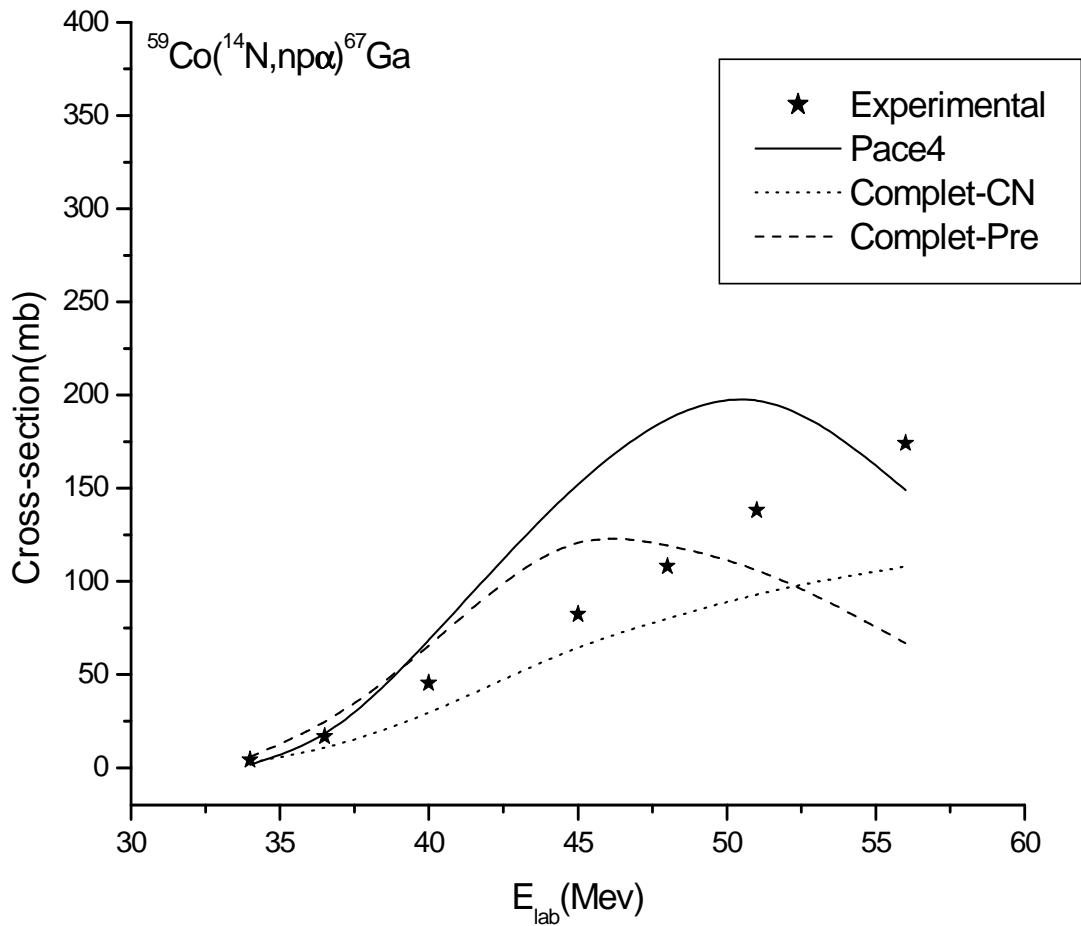


Fig.4.8 Excitation function for the $^{59}\text{Co}(^{14}\text{N},n\text{p}\alpha)^{67}\text{Ga}$ reaction

As shown in Fig. 4.9, for the $^{59}\text{Co}(^{14}\text{N},2p\alpha)^{67}\text{Zn}$ reaction, the complet code gives good results at lower energies. At higher energies, both codes give lower results than experimental results. So we can assume the break-up of the projectile into α and ^{10}B , where ^{10}B fuses with the target nucleus forming the excited state $^{69}\text{As}^*$ and the excited state $^{69}\text{As}^*$ emits two protons, leaving behind the residual nucleus ^{67}Zn . Here the contributions coming from the incomplete fusion reaction are inferred to resolve the discrepancy between the experimentally measured results and the theoretical calculations, which do not take the incomplete fusion reaction into account.

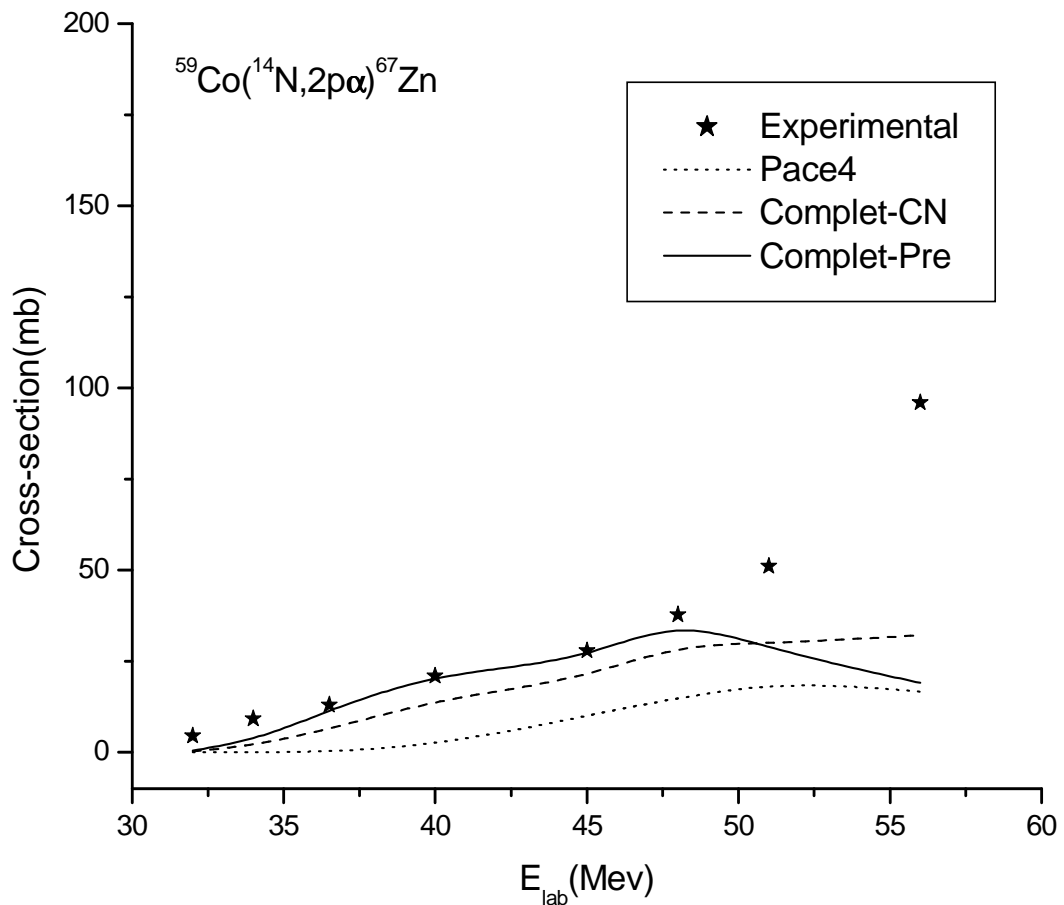


Fig.4.9 Excitation function for the $^{59}\text{Co}(^{14}\text{N},2p\alpha)^{67}\text{Zn}$ reaction

In the $^{59}\text{Co}(^{14}\text{N},2n2p)^{69}\text{Ge}$ reaction, theoretically obtained, especially pace4, results are comparable to the experimentally measured data. So in this reaction the projectile is assumed to fuse completely with the target nucleus forming the excited state $^{73}\text{Se}^*$, and this excited state emits two neutrons and two protons, during the thermalization, leaving behind the residual nucleus ^{69}Ge . For this reaction the complete fusion reaction and pre-equilibrium emission contributions are more pronounced, and the discrepancy in experimentally measured cross-sections and theoretically calculated ones is less.

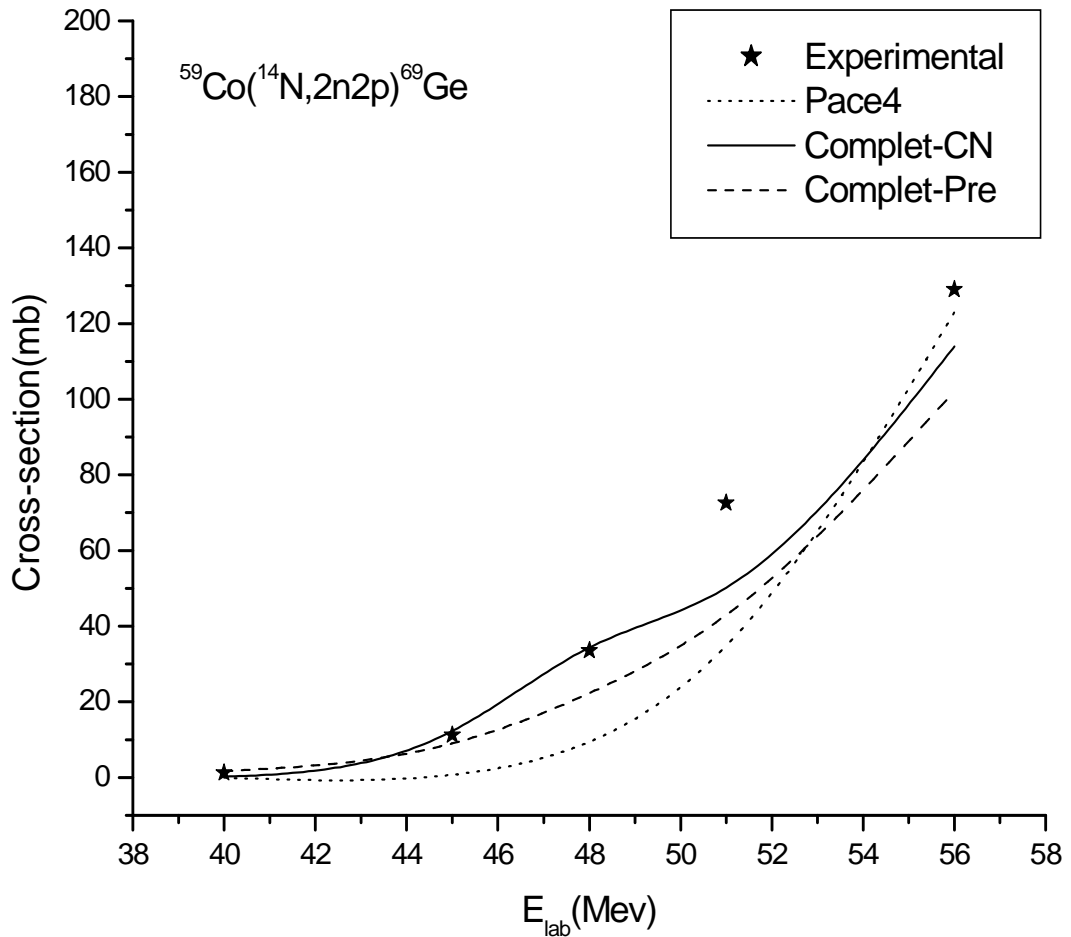


Fig.4.10 Excitation function for the $^{59}\text{Co}(^{14}\text{N},2n2p)^{69}\text{Ge}$ reaction

As clearly shown in Fig. 4.11, for the $^{59}\text{Co}(^{14}\text{N},n2\alpha)^{64}\text{Zn}$ reaction, experimental results are much higher, at higher energies, than the theoretically calculated results using both codes. In this reaction the disagreement between the experimental and theoretical result can be resolved by assuming the projectile to break-up into 2α and ^6Li , where ^6Li fuses with the target nucleus forming the excited state $^{65}\text{Zn}^*$. The excited state $^{65}\text{Zn}^*$ then emits one neutron leaving behind the residual nucleus ^{64}Zn . Here, particularly, the contributions coming from the incomplete fusion reaction are more pronounced at higher energies.

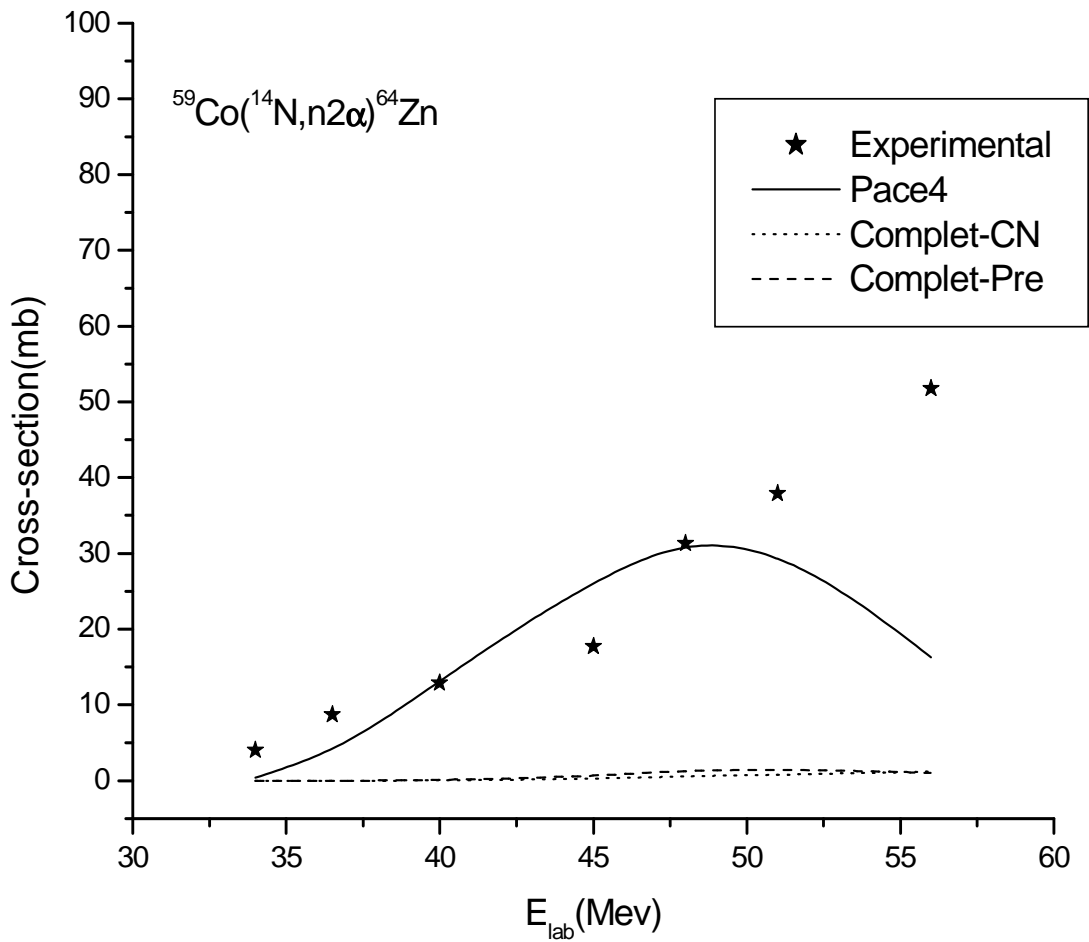


Fig.4.11 Excitation function for the $^{59}\text{Co}(^{14}\text{N},n2\alpha)^{64}\text{Zn}$ reaction

For the $^{59}\text{Co}(^{14}\text{N},3\text{np})^{69}\text{As}$ reaction, theoretical calculations are almost comparable at higher energies with experimental data. From this observation, it is possible to explain this reaction as the complete fusion of the projectile with target. The reaction forms the excited state $^{73}\text{Se}^*$, where this excited state emits three neutrons and one proton leaving behind the residual nucleus ^{69}As . In this reaction the contribution coming from complete fusion is more dominant. It can be seen from this figure that the experimentally measured excitation function is close to the calculated theoretical excitation function if pre-equilibrium emission is included in the calculations. As such it may be possible to say that there is a substantial pre-equilibrium emission at higher energies.

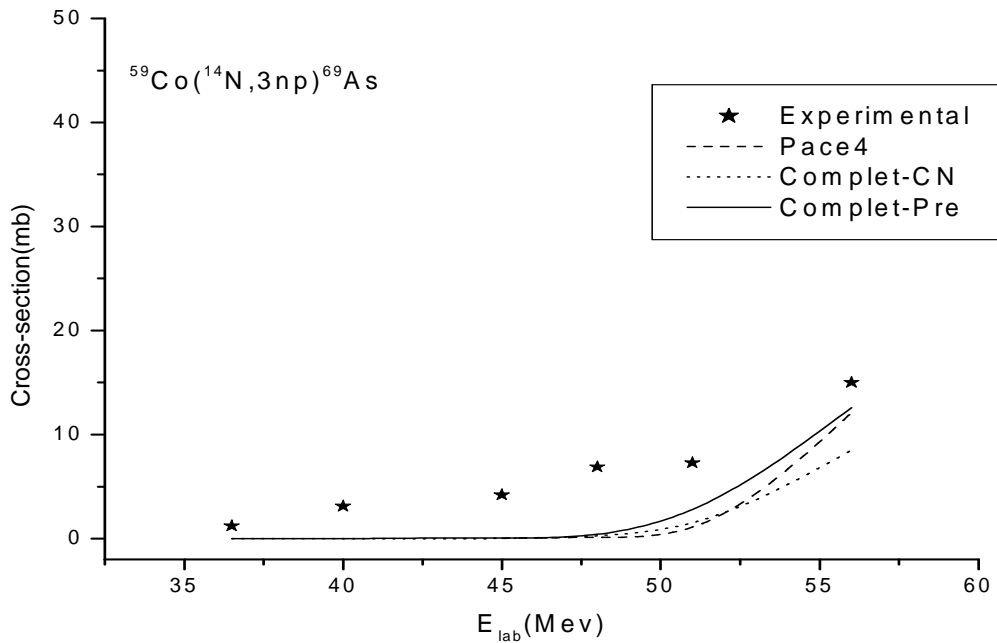


Fig.4.12 Excitation function for the $^{59}\text{Co}(^{14}\text{N},3\text{np})^{69}\text{As}$ reaction

It has been observed that theoretically calculated excitation functions for all the reactions presently studied with the above set of parameters have their maxima shifted towards the lower energies as compared to the experimental data. This is expected as in heavy ion induced reactions the projectile imparts large angular momentum to the composite system. As such, this high angular momentum imparted to the composite system, may inhibit particle emission in the lower by de-excitation. As a result, the peaks of the experimental excitation functions corresponding to a particle emission mode are expected to be shifted towards higher energies.

5. Conclusion

It has been observed, from the above results and discussions that theoretically calculated excitation functions for all the reactions in the system $^{14}\text{N}+^{59}\text{Co}$ presently studied have lower cross-sections compared to the experimentally measured data, particularly at higher energies. This is because, in the theoretical calculations, the contribution from the incomplete fusion reaction is not taken into account. The discrepancy in the experimentally measured excitation functions and the theoretically calculated counter parts may be attributed to the incomplete fusion process. So it may be possible to conclude that complete fusion, incomplete fusion and pre-equilibrium emission processes play important roles in the reactions induced by heavy ions.

From the analysis given by the `pace4` and `complet` codes, it is also possible to conclude that, as observed in this study, for medium (light) mass targets, α emission from the excited system is quite possible. This is because the coulomb barrier is not as such high enough to prevent the emission of α -particles. The enhancement of the experimentally measured cross-sections for alpha emission channels over their theoretical predictions have been attributed to the fact that these residues are not only formed by the complete fusion but also through incomplete fusion.

References

1. P.E.Hodgson, E.Gadioli and E.GadioliErba, Introductory Nuclear Physics, Oxford University Press, 2003.
2. Unnati, M.K.Sharma, B.P.Singh, S.Gupta, H.D.Bhardwaj, A.K.Sinha, International Journal of Modern Physics E, 2005.
3. M.K.Sharma, Unnati, B.K.Sharma, B.P.Singh, H.D.Bhardwaj, R.Kumar, K.S.Golda, and R.Prasad, Physical Review 70, 2004.
4. R. Prasad, D.P. Singh, A. Yadav, P.P.Singh, Unnati, M.K.Sharma, B.P.Singh, R.Kumar and K.S.Golda, ADS/P4-02, India.
5. Exfor library: <http://www.nndc.bnl.gov/exfor>.
6. J.Ernst, Institute for Solid State and Nuclear Physics, The Complet Code library:Complet.for; 445, Germany, 1997.
7. Walter E.Meyerhof, Elements of Nuclear Physics, McGraw-Hill,Inc, 1967.
8. B. Jean-Louis, R. James, S. Michel, Fundamentals in Nuclear Physics, Springer, 2004.
9. J.S.Lilley, Nuclear physics principles and Applications, John Wiley&Sons Ltd, 2001.
10. B. Bindu Kumar nad S. Mukherjee, Physical review C57, 1998.
11. C. Beck, F. A. Souza, N. Rowley, S. J. Sanders, N. Aissaoui, E. E. Alonso, P. Bednarczyk, N. Carlin, S. Courtin, A. Diaz-Torres, A. Dummer, F. Haas, A. Hachem, K. Hagino, F. Hoellinger, R. V. F. Janssens, N. Kintz, R. Liguori Neto, E. Martin, M. M. Moura, M. G. Munhoz, P. Papka, M. Rousseau, A. Sa`nchez i Zafra, O. Ste´zowski, A. A. Suaide, E. M. Szanto, A. Szanto de Toledo, S. Szilner, and J. Takahashi, Physical review C67, 2003.
12. K.F.Amanuel, PHD thesis, Addis Ababa University, Addis Ababa, Ethiopia, 2011.

Declaration

This thesis is my original work, has not been presented for a degree in any other University and that all the sources of material used for the thesis have been dully acknowledged.

Name: Biniyam Nigussie

Signature: _____

Place and time of submission: Addis Ababa University, June 2012

This thesis has been submitted for examination with my approval as University advisor.

Name: Prof.A.K. Chaubey

Signature: _____